

ANALYSES OF THE CONTOUR INTEGRAL METHOD FOR TIME FRACTIONAL SUBDIFFUSION-NORMAL TRANSPORT EQUATION*

FUGUI MA¹, LIJING ZHAO², WEIHUA DENG¹ AND YEJUAN WANG¹

Abstract. In this work, we theoretically and numerically discuss the time fractional subdiffusion-normal transport equation, which depicts a crossover from sub-diffusion (as $t \rightarrow 0$) to normal diffusion (as $t \rightarrow \infty$). Firstly, the well-posedness and regularities of the model are studied by using the bivariate Mittag-Leffler function. Theoretical results show that after introducing the first-order derivative operator, the regularity of the solution can be improved in substance. Then, a numerical scheme with high-precision is developed no matter the initial value is smooth or non-smooth. More specifically, we use the contour integral method (CIM) with parameterized hyperbolic contour to approximate the temporal local and non-local operators, and employ the standard Galerkin finite element method for spacial discretization. Rigorous error estimates show that the proposed numerical scheme has spectral accuracy in time and optimal convergence order in space. Besides, we further improve the algorithm and reduce the computational cost by using the barycentric Lagrange interpolation. Finally, the obtained theoretical results as well as the acceleration algorithm are verified by several 1-D and 2-D numerical experiments, which also show that the numerical scheme developed in this paper is effective and robust.

2020 Mathematics Subject Classification. 35R11 35B65 65D30 65M15.

dates will be set by the publisher.

1. INTRODUCTION

In recent years, the study of fractional diffusion equations (FDEs) has aroused an upsurge (see cf. [1, 3, 8–10], etc.). One class of the most popular FDEs is the time fractional diffusion equations (TFDEs), which are closely related to the time-changing processes. Subordinator is a powerful tool to describe such time-changing process. A subordinator $\mathbb{S} = \{\mathbb{S}_t; t \geq 0\}$ with $\mathbb{S}(0) = 0$ is a stochastic process in continuous time with non-decreasing paths for which $\mathbb{E}[e^{-\lambda \mathbb{S}_t}] = e^{-t\phi(\lambda)}$, $\lambda > 0$ where ϕ is a Bernstein function, whose inverse (or hitting time) process is defined as $\mathbb{E}_t = \inf\{s > 0; \mathbb{S}_s > t\}$. When ϕ is taken as λ^β with $0 < \beta < 1$, the related subordinator is called the β -stable subordinator and its corresponding inverse process is called the inverse β -stable subordinator (see cf. [4, 5], and the references therein).

Denote $\{\bar{\mathbb{S}}_t; t \geq 0\}$ be a drift-less subordinator with Laplace exponent Bernstein function $\phi_0(\lambda) = \int_0^\infty (1 - e^{-\lambda x})\nu(dx)$ and infinite Lévy measure ν . Let \mathbb{E}_t be the inverse process or hitting time process of the β -stable

Keywords and phrases: Time fractional equations; contour integral method; regularity analysis; error estimates; acceleration algorithm.

* *Corresponding author:* Lijing Zhao, e-mail: zhaolj17@nwpu.edu.cn.

¹ School of Mathematics and Statistics, Gansu Key Laboratory of Applied Mathematics and Complex Systems, Lanzhou University, Lanzhou 730000, Peoples Republic of China.

² a. Research and Development Institute of Northwestern Polytechnical University in Shenzhen. b. School of Mathematics and Statistics, Northwestern Polytechnical University, Xian, 710129, Peoples Republic of China.

subordinator $\mathbb{S}_t = Kt + \bar{\mathbb{S}}_t$, $K \geq 0$ ($K = 0$ is drift-less). Then its Laplace exponent Bernstein function ϕ has the following representation

$$\phi(\lambda) = K\lambda + \int_0^\infty (1 - e^{-\lambda x})\nu(dx).$$

Let $u(t, r) = \mathbb{E}_r[u_0(\mathbf{B}_{\mathbb{S}_t})]$ be a subordinated stochastic process where u_0 is a given initial distribution and $\mathbf{B}(t)$ be Brownian motion on \mathbb{R}^d ($d = 1, 2, 3$). Then this stochastic process satisfies the following governing equation [4]:

$$K \frac{d}{dt} u(t, r) + \partial_t^\beta u(t, r) = \Delta u(t, r),$$

which can be widely used to describe many diffusion phenomena in physics, porous medium and hydrology, as well as the reactions or mechanisms in chemistry, engineering, finance and social sciences (see cf. [8–11] and the references therein). Indeed, when $K = 0$, the above equation describes a sub-diffusion process; while if $K > 0$, it depicts a crossover from sub-diffusion diffusion (as $t \rightarrow 0$) to normal diffusion (as $t \rightarrow \infty$), which we shall explain later in detail.

In this paper, we consider a more general time fractional subdiffusion-normal transport model

$$\begin{cases} K \frac{d}{dt} u(t, r) + \partial_t^\beta u(t, r) + Au(t, r) = f(t, r), & \text{in } (t, r) \in (0, T] \times \Omega, \\ u(0, r) = u_0, \end{cases} \quad (1)$$

where $f(t, \cdot): [0, T] \rightarrow L^2(\Omega)$ is a given source term, Ω is a bounded convex polygonal domain in \mathbb{R}^d ($d = 1, 2, 3$) with a boundary $\partial\Omega$, $T > 0$ is a given time value, $K \geq 0$ is a constant, $A := -\Delta: H_0^1(\Omega) \cap H^2(\Omega) \rightarrow L^2(\Omega)$ is the negative Laplacian operator with zero Dirichlet boundary conditions, $\partial_t^\beta u$ is the fractional Caputo derivative which is given in terms of the Riemann-Liouville one (see cf. [3, 4], etc.) by

$$\partial_t^\beta u(t, r) = \frac{1}{\Gamma(\beta)} \frac{d}{dt} \int_0^t (t-s)^{\beta-1} (u(s, r) - u(0, r)) ds$$

with $0 < \beta < 1$ and $\Gamma(\cdot)$ being the Euler Gamma function: $\Gamma(\lambda) = \int_0^\infty t^{\lambda-1} e^{-t} dt$.

In the past two decades, a great deal of studies have been focused on the drift-less case $K = 0$, which include theoretical analyses and numerical computations. In theory, the existing works primarily analyze the well-posedness and regularity of the solution (see cf. [1, 6, 43], etc.). Numerically, researchers consider on how to effectively approximate the time non-local operators. At present, popular numerical discretization mainly include the following categories: L_1 -type methods (see cf. [13, 15, 16, 22, 36], etc); convolution quadrature (CQ) methods (see cf. [17, 19, 20, 37], etc), and other improved versions based on these (see cf. [21, 23, 24, 39], etc.).

For $K > 0$, Problem (1) is expected to improve the modeling delicacy in depicting the anomalous diffusion. In particular, when $K = 1$, Problem (1) is the so-called time-fractional mobile-immobile transport model, which can describe the mechanical behavior of anomalous diffusion transport in heterogeneous porous media fine (see [10, 11], etc). In [4], the author analyzes the existence and uniqueness of the solution from the perspective of probability theory by using random representation; based on some given regularity assumptions, [45] uses the CQ method and the radial basis function-generated finite difference method to solve Problem (1); for $K = 1$, [39] proposes a second-order accurate L_1 scheme over non-uniform time steps, and [44] develops the averaged L_1 compact difference scheme, etc. To the best of our knowledge, the present works on numerical approximation, well-posedness and regularity analysis for Problem (1) are still limited.

From the works list above, we can see that, compared with theoretical analyses, numerical computations for TFDEs are predominant. Although some high-order schemes have been proposed, strong regularity of solutions should be required at the same time (see Table 1), which is inconsistent with the regularity of the physical model itself. Besides, due to the historical dependence of the time non-local operators and its weak singularity at the original point, the storage and computational costs of the traditional numerical schemes are usually expensive. This paper targets on: (i) the study of the well-posedness of Problem (1) for $K > 0$ and the regularity of its

TABLE 1. Part summary of convergence rates and regularity assumptions in time for existing time semi-discrete schemes of Problem (1) when $K = 0$, where τ is the time discrete step-spacing.

method	rate	regularity assumption
[13]	$\mathcal{O}(\tau)$	$\forall x \in \Omega, u$ is C^2 in t .
[15]	$\mathcal{O}(\tau^{3-\beta})$	$\forall x \in \Omega, u$ is C^3 in t .
[16]	$\mathcal{O}(\tau^{2-\beta})$	$\forall x \in \Omega, u$ is C^2 in t .
[20]	$\mathcal{O}(\tau^{2-\beta})$	$\forall x \in \Omega, u$ is C^2 in t .
[22]	$\mathcal{O}(\tau^{2-\beta})$	$\forall x \in \Omega, u$ is C^2 in t .
[21]	$\mathcal{O}(\tau^2)$	$\forall x \in \Omega, u$ is C^2 in t .
[23]	$\mathcal{O}(\tau^2)$	$\forall x \in \Omega, u$ is C^3 in t .

solution from the perspective of PDE. (ii) high-performance numerical method with low regularity and $\mathcal{O}(1)$ storage requirements in temporal direction. (iii) algorithm acceleration to reduce the computational operations.

To illustrate the time semi-discrete method, we consider the following time-fractional initial-boundary value problem (i.e., Problem (1) with $K = 0$)

$$\partial_t^\beta u(t, r) + Au(t, r) = f(t, r) \text{ with } u(0, r) = u_0. \quad (2)$$

Based on the fact that the spectrum of A is constrained in a sufficiently small sector, i.e.,

$$sp(A) \subset \Sigma_\theta := \{z \in \mathbb{C} : z \neq 0, |\arg(z)| < \theta\} \text{ with } \theta \in (0, \pi/2),$$

and the resolvent $(zI + A)^{-1} : L^2(\Omega) \rightarrow L^2(\Omega)$ satisfies (see [28, Theorem 3.7.11])

$$\|(zI + A)^{-1}\|_{L^2(\Omega)} \leq \frac{C}{1 + |z|} \quad \text{for all } z \in \Sigma_\theta, \theta \in (\pi/2, \pi). \quad (3)$$

the construction of the time semi-discrete method mainly contains two steps (for convenience, we will ignore the spatial variable identifier in the sequence, i.e., $u(t) := u(t, r)$, $f(t) := f(t, r)$) :

Step I: Under weak restrictions on $u(t)$, there exists a positive constant σ_0 ($\sigma_0 > 0$ is often referred to as the convergent abscissa), such that the Laplace transform $\hat{u}(z)$ exists for $\text{Re}(z) > \sigma_0$ (i.e., there is $C > 0$, $|u(t)| \leq Ce^{\sigma_0 t}$) (see [32]), we express the solution $u(t)$ in the form of

$$u(t) = \frac{1}{2\pi i} \int_{\sigma - i\infty}^{\sigma + i\infty} e^{zt} \hat{u}(z) dz, \quad \text{Re}(z) > \sigma_0, \quad (4)$$

and

$$\hat{u}(z) = (z^\beta I + A)^{-1} (z^{\beta-1} u_0 + \hat{f}(z)).$$

Step II: Propose an efficient numerical method to approximate the improper integral (4). Attracted by the simplicity and efficiency of the contour integral method (CIM) (cf. [25, 27, 31, 32]), we further develop it in this paper. Other numerical methods for the improper integrals can see cf. [29, 30], etc.

The basic idea of CIM is, by Cauchy's integral theorem, the original integration path of the inverse Laplace transform (is a vertical line from negative infinity to positive infinity) can be deformed into a contour with $\text{Re}(z) \rightarrow -\infty$ at each end. Thus, the exponential factor e^{zt} can force a rapid decay of the integrand on the contour, which is greatly beneficial to the fast convergence of the numerical computation to the improper integral (4), and avoiding the unfeasible approximation on the vertical line as well as high frequency oscillation.

Let such an appropriate contour be parameterized by

$$\Gamma : z = z(\phi), \quad -\infty < \phi < \infty. \quad (5)$$

Then the solution (4) can be rewritten as

$$u(t) = \frac{1}{2\pi i} \int_{-\infty}^{\infty} e^{z(\phi)t} \widehat{u}(z(\phi)) z'(\phi) d\phi. \quad (6)$$

Approximating integral (6) by mid-point rule with uniform step-spacing τ , we can get

$$u(t) \approx u^N(t) = \frac{\tau}{2\pi i} \sum_{k=-\infty}^{\infty} e^{z(\phi_k)t} \widehat{u}(z(\phi_k)) z'(\phi_k), \quad (7)$$

where $\phi_k = (k + 1/2)\tau$ (if trapezoidal rule is used, $\phi_k = k\tau$). Suppose that the contour Γ is symmetric with respect to the real axis and Laplace transform of $f(t)$ holds (by Riemann-Schwartz reflection principle, there is $\widehat{f}(\bar{z}) = \overline{\widehat{f}(z)}$), then we have $\widehat{u}(\bar{z}) = \overline{\widehat{u}(z)}$. After truncating, there is

$$u(t) \approx u^N(t) = \frac{\tau}{\pi} \operatorname{Im} \left\{ \sum_{k=0}^{N-1} e^{z(\phi_k)t} \widehat{u}(z(\phi_k)) z'(\phi_k) \right\}. \quad (8)$$

To our knowledge, CIM is early proposed and discussed in [31], and improved and applied by cf. [25–27, 32], etc. Comparing with other traditional numerical methods, CIM, which is spectral accurate and cheap in computation, can belittle the influence of the singularity at the origin, and requires low regularity of the solution. What is more, to compute the solution value at a current moment by CIM, it does not depend on the information on history, and so can perform parallel computing.

The main contributions of this paper are listed as follows:

- Firstly, we discuss the well-posedness and regularities of the new model (1), both in temporal as well as spatial directions, by use of the bivariate Mittag-Leffler function, and get some novel results (see Subsec. 2.3.2).
- Secondly, we develop a numerical scheme for the time fractional subdiffusion-normal problem (1) by using the standard Galerkin FEM with continuous piecewise linear functions for space discretization and CIM with parameterized hyperbolic contour for time discretization.
- We show the error analysis and optimal convergence estimation in detail. Spacial second-order convergence rate can be reached no matter the initial data is smooth or non-smooth. The optimal parameters determining the shape of the contour in CIM are given.
- Finally, we develop an acceleration algorithm based on the barycentric Lagrange interpolation approximation, and take several numerical experiments with smooth as well as non-smooth initial data in 1-D and 2-D to demonstrate the efficiency and robustness of our proposed numerical scheme.

The rest of this paper is organized as follows: in Sec. 2, the well-posedness and regularity of the solution are discussed; in Sec. 3 and 4, the time and space semi-discrete methods are proposed respectively; in Sec. 5, the fully discrete scheme of Problem (1) is established and the convergence analysis is performed; in Sec. 6, an acceleration algorithm for CIM and its error estimation are presented; in Sec. 7, numerical experiments are given to demonstrate the theoretical results; some conclusions are made in Sec. 8.

2. SMOOTHNESS THEORY

2.1. Preliminaries

We begin by introducing some notations about functional spaces that will be adopted in the subsequent. As we have indicated already in Sec. 1, the operator A is the negative Laplacian with zero Dirichlet boundary condition. Let $(\lambda_j, \varphi_j)_{j \in \mathbb{N}}$ be the eigenvalues of A ordered non-decreasingly and the corresponding eigenfunctions

normalized in the $L^2(\Omega)$ norm. Then the fractional Sobolev space $\dot{H}^q(\Omega)$ ($q \geq 0$) is defined as (see cf. [34], etc)

$$\dot{H}^q(\Omega) := \{v \in L^2(\Omega) : \sum_{j=1}^{\infty} \lambda_j^q(v, \varphi_j)^2 < \infty\}$$

with the following scalar product and norm

$$(u, v)_{\dot{H}^q(\Omega)} := \sum_{j=1}^{\infty} \lambda_j^q(u, \varphi_j)(v, \varphi_j), \quad \|v\|_{\dot{H}^q(\Omega)} := (v, v)_{\dot{H}^q(\Omega)}^{1/2} \quad \forall u, v \in \text{span}\{\varphi_j\}.$$

It is clear that $\dot{H}^0(\Omega) = L^2(\Omega)$, $\dot{H}^1(\Omega) = H_0^1(\Omega)$ and $\dot{H}^2(\Omega) = H_0^1(\Omega) \cap H^2(\Omega)$.

We also define the dual space of $\dot{H}^q(\Omega)$ as

$$\dot{H}^{-q}(\Omega) := \{v \in L^2(\Omega) : \sum_{j=1}^{\infty} \lambda_j^{-q}(v, \varphi_j)^2 < \infty\}$$

with norm

$$\|v\|_{\dot{H}^{-q}(\Omega)} := (v, v)_{\dot{H}^{-q}(\Omega)}^{1/2} \quad \text{and} \quad (u, v)_{\dot{H}^{-q}(\Omega)} := \sum_{j=1}^{\infty} \lambda_j^{-q}(u, \varphi_j)(v, \varphi_j).$$

For $q \geq 0$, there is $\dot{H}^q(\Omega) \subset L^2(\Omega) \subset \dot{H}^{-q}(\Omega)$ (see cf. [7], etc.).

Besides, for $\theta \in (\pi/2, \pi)$, we define another sector

$$\Sigma_{\theta, \delta} := \{z \in \mathbb{C} : |z| \geq \delta > 0, |\arg(z)| < \theta\},$$

and an integral contour $\Gamma_{\theta, \delta} \subset \mathbb{C}$

$$\Gamma_{\theta, \delta} := \{z \in \mathbb{C} : |z| = \delta, |\arg(z)| \leq \theta\} \cup \{z \in \mathbb{C} : z = re^{\pm i\theta}, 0 < \delta \leq r < \infty\},$$

which oriented with an increasing imaginary part and $i^2 = -1$.

Next, we perform the well-posedness and regularity analysis of Problem (1). Before this, we remark that throughout this paper c and C denote positive constants, not necessarily the same at different occurrences, which are independent of the functions involved.

2.2. Representation of solution

Let $u(t)$ be the solution of Problem (1). Take Laplace transform on the equation in (1) and perform simple operations [3], we get

$$((Kz + z^\beta)I + A)\hat{u}(z) = (K + z^{\beta-1})u_0 + \hat{f}(z). \quad (9)$$

Denote

$$\eta(z) := Kz + z^\beta \quad \text{and} \quad W(z) := \frac{\eta(z)}{z}(\eta(z)I + A)^{-1}. \quad (10)$$

Then Eq. (9) can be rewritten as

$$\hat{u}(z) = W(z)u_0 + z\eta^{-1}(z)W(z)\hat{f}(z). \quad (11)$$

Transforming the inverse Laplace transform, the solution $u(t)$ can be expressed as

$$u(t) = \frac{1}{2\pi i} \int_{\sigma_0 - i\infty}^{\sigma_0 + i\infty} e^{zt} \hat{u}(z) dz, \quad \text{Re}(z) > \sigma_0. \quad (12)$$

From Remark 2.1 below, the integrand $\hat{u}(z)$ in Eq. (12) is analytical for $z \in \Sigma_{\theta, \delta}$ and any $\delta > 0$. Therefore, we can deform the integral contour from $\sigma_0 + i\mathbb{R}$ to $\Gamma_{\theta, \delta}$, which reads

$$u(t) = \frac{1}{2\pi i} \int_{\Gamma_{\theta, \delta}} e^{zt} \hat{u}(z) dz \quad \text{with } \theta \in (\pi/2, \pi). \quad (13)$$

We formally name the above solution as the mild solution of Problem (1).

Remark 2.1. The integrand function $\hat{u}(z)$ in Eq. (12) is analytical for $z \in \Sigma_\theta$ with $\theta \in (\pi/2, \pi)$. In fact, according to the expression of $\hat{u}(z)$ in Eq. (11), there are two possible cases that may cause singularity: one is $z^{\beta-1}$; another is the operator $(\eta(z)I + A)^{-1}$. For the previous one, obviously, $z = 0$ is a singularity point. As for $(\eta(z)I + A)^{-1}$, singularity occurs only if $\operatorname{Re} \eta(z) = -\lambda_j < 0$ and $\operatorname{Im} \eta(z) = 0$ are satisfied at the same time. But, it is impossible. Because, by letting $z = re^{i\zeta}$, $r \geq 0$ and $\zeta \in [0, \pi]$, it can be seen that when $r = 0$ or $\zeta = 0$, there is $\operatorname{Im} \eta(z) = Kr \sin \zeta + r^\beta \sin(\beta\zeta) = 0$, while $\operatorname{Re} \eta(z) = Kr \cos \zeta + r^\beta \cos(\beta\zeta) \geq 0$, which contraries to $\operatorname{Re} \eta(z) < 0$. Thus, $\hat{u}(z)$ is only singular at $z = 0$ and analytic for $z \in \Sigma_\theta$, with $\theta \in (\pi/2, \pi)$.

Proposition 2.2. Let $\eta(z)$ and $W(z)$ be defined in Eq. (10), and let $\delta > \max \{1, (\frac{2}{K})^{1/(1-\beta)}\}$ be large enough. For $K > 0$, we have the following assertions,

(I): for fixed $\theta' \in (\frac{2\pi}{3}, \pi)$, there are $\eta(z) \in \Sigma_\theta$ with $\theta \in (\frac{\pi}{2}, \pi)$ and

$$c|z| < |\eta(z)| \leq C|z| \text{ for all } z \in \Sigma_{\theta', \delta}. \quad (14)$$

(II): the operator $W(z): L^2(\Omega) \rightarrow L^2(\Omega)$ is well-defined and bounded for $z \in \Sigma_{\theta', \delta}$, and satisfies

$$\|W(z)\|_{L^2(\Omega)} \leq C|z|^{-1} \text{ and } \|AW(z)\|_{L^2(\Omega)} \leq C. \quad (15)$$

Proof. For (I), according to the condition that δ satisfies, for all $z \in \Sigma_{\theta', \delta}$, there holds

$$\sin(|\arg(Kz + z^\beta) - \arg(Kz)|) \cdot K|z| \leq |z|^\beta.$$

Therefore,

$$|\arg(Kz + z^\beta) - \arg(Kz)| \leq \arcsin\left(\frac{1}{K|z|^{1-\beta}}\right) \leq \arcsin\left(\frac{1}{K\delta^{1-\beta}}\right) < \frac{\pi}{6}.$$

Consequently, if $z \in \Sigma_{\theta'}$, $\theta' \in (\frac{2\pi}{3}, \pi)$, then $\eta(z)$ belongs to Σ_θ with $\theta \in (\frac{\pi}{2}, \pi)$. In addition, for all $z \in \Sigma_{\theta', \delta}$, we have

$$\frac{|Kz + z^\beta|}{|z|} \leq \frac{K|z| + |z|^\beta}{|z|} \leq K + \frac{1}{|z|^{1-\beta}} \leq C$$

and

$$\frac{|Kz + z^\beta|}{|z|} \geq \frac{|K|z| - |z|^\beta}{|z|} \geq \frac{K}{2}.$$

Therefore, we obtain that $c|z| \leq |\eta(z)| \leq C|z|$. The proof of the Proposition 2.2(I) is completed.

For (II), by Proposition 2.2 (I), for $z \in \Sigma_{\theta', \delta}$, there holds $\eta(z) \in \Sigma_\theta$. Therefore, the resolvent estimation of operator $(\eta(z)I + A)^{-1}$ (see Eq. (3)) satisfies

$$\|(\eta(z)I + A)^{-1}\|_{L^2(\Omega)} \leq \frac{C}{1 + |\eta(z)|}.$$

Let

$$z\eta^{-1}(z)(\eta(z)I + A)\phi = \psi,$$

which can be reformulated as

$$(\eta(z)I + A)\phi = z^{-1}\eta(z)\psi,$$

and thus

$$\phi = z^{-1}\eta(z)(\eta(z)I + A)^{-1}\psi.$$

By the resolvent estimation mentioned above, we then have

$$\|\phi\|_{L^2(\Omega)} \leq C|z|^{-1}\|\psi\|_{L^2(\Omega)}.$$

Now we can deduce that the operator $W(z) : L^2(\Omega) \rightarrow L^2(\Omega)$ is well-defined and bounded. Moreover, since $A(\eta(z)I + A)^{-1} = I - \eta(z)(\eta(z)I + A)^{-1}$, by Proposition 2.2 (I), there also holds

$$\|AW(z)\|_{L^2(\Omega)} = \|z^{-1}\eta(z) - z^{-1}\eta(z)\eta(z)(\eta(z)I + A)^{-1}\|_{L^2(\Omega)} \leq C.$$

The proof of this proposition is completed. \square

Here, we remark that unless otherwise specified, when $z \in \Sigma_{\theta, \delta}$, θ is always selected as $\theta \in (\frac{2\pi}{3}, \pi)$ and δ satisfies the condition mentioned in Proposition 2.2.

2.3. Solution theory

In this subsection, we shall analyze the well-posedness and regularity of Problem (1) with $K > 0$. For the case of $K = 0$, one can refer to the literature [7, 12, 43], etc..

2.3.1. Well-posedness and regularity

Since $\{(\lambda_j, \varphi_j)\}_{j \in \mathbb{N}}$ are the eigenvalues ordered non-decreasingly and the normalized eigenfunctions of A , there holds

$$-\Delta \varphi_j = \lambda_j \varphi_j \text{ in } \Omega, \text{ and } \varphi_j = 0 \text{ on } \partial\Omega, \text{ for all } j \in \mathbb{N}_+. \quad (16)$$

By using the standard separation of variables and eigenvalue expansions, Problem (1) reduces to the following initial value problem

$$K \frac{\partial}{\partial t} u_j(t) + \partial_t^\beta u_j(t) + \lambda_j u_j(t) = (f(t), \varphi_j) \text{ with } u_{j,0} = (u_0, \varphi_j), \text{ for all } j \in \mathbb{N}_+. \quad (17)$$

Taking Laplace transform for the above problem, and combining

$$\frac{K + z^{\beta-1}}{Kz + z^\beta + \lambda_j} = \frac{z^{-1}}{1 + \frac{1}{K}z^{\beta-1} + \frac{\lambda_j}{K}z^{-1}} + \frac{1}{K} \cdot \frac{z^{\beta-2}}{1 + \frac{1}{K}z^{\beta-1} + \frac{\lambda_j}{K}z^{-1}},$$

with the operational method in fractional calculus mentioned in Ref. [38], the solution $u(t)$ of problem (1) can be formally represented by

$$u(t) = E(t)u_0 + \int_0^t \overline{E}(t-\tau)f(\tau)d\tau, \quad (18)$$

where

$$\overline{E}(t)\chi := \sum_{j=1}^{\infty} E_{(1-\beta,1),1}^1 \left(\frac{-1}{K}t^{1-\beta}, \frac{-\lambda_j}{K}t \right) (\chi, \varphi_j)\varphi_j, \quad (19)$$

$$E(t)\chi := \sum_{j=1}^{\infty} \left[E_{(1-\beta,1),1}^1 \left(\frac{-1}{K}t^{1-\beta}, \frac{-\lambda_j}{K}t \right) + \frac{1}{K}t^{1-\beta} E_{(1-\beta,1),2-\beta}^1 \left(\frac{-1}{K}t^{1-\beta}, \frac{-\lambda_j}{K}t \right) \right] (\chi, \varphi_j)\varphi_j, \quad (20)$$

and $E_{(\alpha,\beta),\gamma}^1(z_1, z_2)$ is the bivariate Mittag-Leffler function defined in Eq. (67), whose properties are shown in the lemmata below (see Appendix B for proofs.).

Lemma 2.3. *For α, β, γ and $\delta \in \mathbb{C}$, if $\operatorname{Re}(\alpha) > 0$ and $\operatorname{Re}(\beta) > 0$, then the bivariate Mittag-Leffler $E_{(\alpha,\beta),\gamma}^\delta(z_1, z_2)$ defined in Eq. (67) is an entire function.*

Lemma 2.4. *Let $\omega_1, \omega_2, \alpha, \beta, \gamma \in \mathbb{R}$ with $0 < \alpha < \beta \leq 1$, $\gamma \geq 0$ and $\omega_1, \omega_2 < 0$. For $t \in [0, \infty)$, there exists a positive constant C , such that*

$$\left| E_{(\alpha,\beta),\gamma}^1(\omega_1 t^\alpha, \omega_2 t^\beta) \right| \leq \frac{C}{1 + |\omega_2 t^\beta|}.$$

Lemma 2.5 (cf. [41]). *Let $\alpha, \beta, \gamma, \omega_1, \omega_2 \in \mathbb{C}$ with $\operatorname{Re}(\alpha), \operatorname{Re}(\beta), \operatorname{Re}(\gamma) > 0$. Then the relationship between fractional calculus of $E_{(\alpha,\beta),\gamma}(\omega_1 t^\alpha, \omega_2 t^\beta)$ and the bivariate Mittag-Leffler function is*

$$D_t^{\mu_1} \left[t^{\gamma-1} E_{(\alpha,\beta),\gamma}^1(\omega_1 t^\alpha, \omega_2 t^\beta) \right] = t^{\gamma-\mu_1-1} E_{(\alpha,\beta),\gamma-\mu_1}^1(\omega_1 t^\alpha, \omega_2 t^\beta),$$

for $\mu_1 \in \mathbb{C}$ (fractional integral if $\operatorname{Re}(\mu_1) < 0$, or fractional derivative if $\operatorname{Re}(\mu_1) \geq 0$), where $D_t^{\mu_1}$ denotes the Riemann-Liouville fractional derivative (integral) defined as $D_t^{\mu_1} u(t) = \frac{1}{\Gamma(\mu_1)} \frac{d^k}{dt^k} \int_0^t (t-\tau)^{\mu_1-1} u(\tau) d\tau$ with $k = \lfloor \operatorname{Re}(\mu_1) \rfloor + 1$.

Remark 2.6. We note that, by the definitions of the two fractional operators D_t^a and ∂_t^a , it is easy to verify when $\gamma \geq 1$ the equation in Lemma 2.5 still holds for the case of Caputo fractional derivative.

Definition 2.7 (cf. [7]). We call $u(\cdot, t)$ a weak solution to Problem (1) with zero Dirichlet boundary condition if (1) holds in $L^2(\Omega)$ and $u(\cdot, t) \in H_0^1(\Omega)$ for almost all $t \in (0, T)$ and $u(\cdot, t) \in C([0, T], \dot{H}^{-p}(\Omega))$, $\lim_{t \rightarrow 0} \|u(\cdot, t) - u_0\|_{\dot{H}^{-p}(\Omega)} = 0$ with $p > 0$.

Now we are ready to give the well-posedness and regularity of the solution to Problem (1).

Theorem 2.8. *Let $0 < \beta < 1$, $K > 0$ and $f \equiv 0$.*

(I): *If $u_0 \in L^2(\Omega)$, then the weak solution $u(t)$ to Problem (1) given in Eq. (18) is unique, satisfying $u(t) \in C^1((0, T]; L^2(\Omega)) \cap C([0, T]; L^2(\Omega)) \cap C((0, T]; H^2(\Omega) \cap H_0^1(\Omega))$, with $\partial_t^\beta u(t) \in C((0, T]; L^2(\Omega))$, and*

$$\begin{cases} \|u(t)\|_{C([0,T],L^2(\Omega))} \leq C \|u_0\|_{L^2(\Omega)}, \\ \|u(t)\|_{\dot{H}^2(\Omega)} + \left\| \frac{d}{dt} u(t) \right\|_{L^2(\Omega)} + t^{\beta-1} \left\| \partial_t^\beta u(t) \right\|_{L^2(\Omega)} \leq C t^{-1} \|u_0\|_{L^2(\Omega)}, \quad t \in (0, T]. \end{cases} \quad (21)$$

(II): *If $u_0 \in H_0^1(\Omega)$, then the unique weak solution $u(t)$ given in Eq. (18) belongs to $C^1((0, T]; L^2(\Omega)) \cap L^2(0, T; H^{2-\varepsilon}(\Omega) \cap H_0^1(\Omega)) \cap C((0, T]; H^2(\Omega) \cap H_0^1(\Omega))$ for any $\varepsilon > 0$, with $\partial_t^\beta u(t) \in C((0, T]; L^2(\Omega)) \cap L^2((0, T) \times \Omega)$, and there exists a positive constant $C > 0$ such that*

$$\begin{cases} \|u(t)\|_{L^2(0,T;H^{2-\varepsilon}(\Omega) \cap H_0^1(\Omega))} \leq C \|u_0\|_{\dot{H}^1(\Omega)}, \\ \|u(t)\|_{C((0,T];\dot{H}^2(\Omega))} + \left\| \frac{d}{dt} u(t) \right\|_{C((0,T];L^2(\Omega))} + t^{\beta-1} \left\| \partial_t^\beta u(t) \right\|_{C((0,T];L^2(\Omega))} \leq C t^{-1/2} \|u_0\|_{\dot{H}^1(\Omega)}. \end{cases} \quad (22)$$

(III): *Furthermore, if $u_0 \in H^2(\Omega) \cap H_0^1(\Omega)$, then the unique weak solution $u(t)$ given in Eq. (18) belongs to $C^1([0, T]; L^2(\Omega)) \cap C([0, T]; H^2(\Omega) \cap H_0^1(\Omega))$, with $\partial_t^\beta u \in C([0, T]; L^2(\Omega))$, and following priori estimate holds:*

$$\|u(t)\|_{C([0,T],\dot{H}^2(\Omega))} + \left\| \frac{d}{dt} u(t) \right\|_{C([0,T];L^2(\Omega))} + \left\| \partial_t^\beta u(t) \right\|_{C([0,T];L^2(\Omega))} \leq C \|u_0\|_{\dot{H}^2(\Omega)}. \quad (23)$$

Proof. Let $f \equiv 0$. By Eq. (18), the mild solution $u(t)$ can be expressed as

$$u(t) = \sum_{j=1}^{\infty} \left[E_{(1-\beta,1),1}^1 \left(\frac{-1}{K} t^{1-\beta}, \frac{-\lambda_j}{K} t \right) + \frac{1}{K} t^{1-\beta} E_{(1-\beta,1),2-\beta}^1 \left(\frac{-1}{K} t^{1-\beta}, \frac{-\lambda_j}{K} t \right) \right] (u_0, \varphi_j) \cdot \varphi_j. \quad (24)$$

For any $p, q \in \mathbb{R}$, $0 \leq p - q \leq 2$, by Lemma 2.4, there holds

$$\|u(t)\|_{\dot{H}^p(\Omega)}^2 = \sum_{j=1}^{\infty} \lambda_j^p \left[E_{(1-\beta,1),1}^1 \left(\frac{-1}{K} t^{1-\beta}, \frac{-\lambda_j}{K} t \right) + \frac{1}{K} t^{1-\beta} E_{(1-\beta,1),2-\beta}^1 \left(\frac{-1}{K} t^{1-\beta}, \frac{-\lambda_j}{K} t \right) \right]^2 |(u_0, \varphi_j)|^2$$

$$\begin{aligned}
&\leq Ct^{-(p-q)} \sum_{j=1}^{\infty} \frac{(\lambda_j t)^{p-q}}{(K + \lambda_j t)^2} \lambda_j^q |(u_0, \varphi_j)|^2 + Ct^{2(1-\beta)-(p-q)} \sum_{j=1}^{\infty} \frac{(\lambda_j t)^{p-q}}{(K + \lambda_j t)^2} \lambda_j^q |(u_0, \varphi_j)|^2 \\
&\leq Ct^{-(p-q)} \sum_{j=1}^{\infty} \lambda_j^q |(u_0, \varphi_j)|^2 + Ct^{2(1-\beta)-(p-q)} \sum_{j=1}^{\infty} \lambda_j^q |(u_0, \varphi_j)|^2 \leq Ct^{-(p-q)} \|u_0\|_{\dot{H}^q(\Omega)}^2, \tag{25}
\end{aligned}$$

where the last second inequality holds because $\sup_{j \in \mathbb{N}} \frac{(\lambda_j t)^{p-q}}{(K + \lambda_j t)^2} \leq C'$ with $0 \leq p - q \leq 2$, and the last inequality holds because $t^{1-\beta} \leq C$ with $0 < \beta < 1$. Similar to the above analysis, thanks to Lemmata 2.4 and 2.5, for all $0 < \mu_1 \leq 1$, there holds

$$\begin{aligned}
&\|\partial_t^{\mu_1} u(t)\|_{\dot{H}^p(\Omega)}^2 \\
&= \sum_{j=1}^{\infty} \lambda_j^p \left[\partial_t^{\mu_1} E_{(1-\beta,1),1}^1 \left(\frac{-1}{K} t^{1-\beta}, \frac{-\lambda_j}{K} t \right) + \frac{1}{K} \partial_t^{\mu_1} \left(t^{1-\beta} E_{(1-\beta,1),2-\beta}^1 \left(\frac{-1}{K} t^{1-\beta}, \frac{-\lambda_j}{K} t \right) \right) \right]^2 |(u_0, \varphi_j)|^2 \\
&\leq Ct^{-(p-q)-2\mu_1} \sum_{j=1}^{\infty} \frac{(\lambda_j t)^{p-q}}{(K + \lambda_j t)^2} \lambda_j^q |(u_0, \varphi_j)|^2 + Ct^{2(1-\beta)-(p-q)-2\mu_1} \sum_{j=1}^{\infty} \frac{(\lambda_j t)^{p-q}}{(K + \lambda_j t)^2} \lambda_j^q |(u_0, \varphi_j)|^2 \\
&\leq Ct^{-(p-q)-2\mu_1} \|u_0\|_{\dot{H}^q(\Omega)}^2. \tag{26}
\end{aligned}$$

With these, the detailed proof of the theorem is as follows:

(a) *Proof of Theorem 2.8 (I).*

Denote

$$E_j(\beta, K, t) := E_{(1-\beta,1),1}^1 \left(\frac{-1}{K} t^{1-\beta}, \frac{-\lambda_j}{K} t \right) + \frac{1}{K} t^{1-\beta} E_{(1-\beta,1),2-\beta}^1 \left(\frac{-1}{K} t^{1-\beta}, \frac{-\lambda_j}{K} t \right)$$

for simplicity. By Eq. (24), we can deduce that for $p = q = 0$,

$$\begin{aligned}
\|u(t)\|_{L^2(\Omega)}^2 &= \sum_{j=1}^{\infty} |E_j(\beta, K, t)|^2 \cdot |(u_0, \varphi_j)|^2 \\
&\leq c \sum_{j=1}^{\infty} \left(\frac{1}{K + \lambda_j t} \right)^2 |(u_0, \varphi_j)|^2 + ct^{2(1-\beta)} \sum_{j=1}^{\infty} \left(\frac{1}{K + \lambda_j t} \right)^2 \cdot |(u_0, \varphi_j)|^2 \leq C \|u_0\|_{L^2(\Omega)}^2, \tag{27}
\end{aligned}$$

and for $p = 2, q = 0$,

$$\|u(t)\|_{\dot{H}^2(\Omega)}^2 = \sum_{j=1}^{\infty} \lambda_j^2 |E_j(\beta, K, t)|^2 \cdot |(u_0, \varphi_j)|^2 \leq Ct^{-2} \|u_0\|_{L^2(\Omega)}^2. \tag{28}$$

Furthermore, by Inequality (26), we have for $\mu_1 = 1$,

$$\left\| \frac{d}{dt} u(t) \right\|_{L^2(\Omega)}^2 = \sum_{j=1}^{\infty} \left| \frac{d}{dt} E_j(\beta, K, t) \right|^2 \cdot |(u_0, \varphi_j)|^2 \leq Ct^{-2} \|u_0\|_{L^2(\Omega)}^2, \tag{29}$$

and for $0 < \beta < 1$,

$$\left\| \partial_t^\beta u(t) \right\|_{L^2(\Omega)}^2 = \sum_{j=1}^{\infty} \left| \partial_t^\beta E_j(\beta, K, t) \right|^2 \cdot |(u_0, \varphi_j)|^2 \leq Ct^{-2\beta} \|u_0\|_{L^2(\Omega)}^2. \tag{30}$$

Consequently, the following assertions can be inferred from the above estimates. Firstly, Inequality (27) indicates that the series $\sum_{j=1}^{\infty} E_j(\beta, K, t)(u_0, \varphi_j)\varphi_j$ is convergent in $L^2(\Omega)$ uniformly for all $t \in [0, T]$, therefore, by Abel Continuity Theorem, $u(t) \in C([0, T]; L^2(\Omega))$. Similarly, we see from Inequality (28) that the series $\sum_{j=1}^{\infty} \lambda_j E_j(\beta, K, t)(u_0, \varphi_j)\varphi_j$ is convergent in $L^2(\Omega)$ uniformly for $t \in [\delta, T]$ and any $\delta > 0$, which implies $Au(t) \in C((0, T]; L^2(\Omega))$, i.e., $u(t) \in C((0, T]; H^2(\Omega) \cap H_0^1(\Omega))$, and from (29) that $u(t) \in C^1((0, T]; L^2(\Omega))$, and from (30) that $\partial_t^\beta u(t)$ belongs to $C((0, T]; L^2(\Omega))$. Together, these results that show the mild solution $u(t)$ belongs to $C^1((0, T]; L^2(\Omega)) \cap C([0, T]; L^2(\Omega)) \cap C((0, T]; H^2(\Omega) \cap H_0^1(\Omega))$, and satisfies $\partial_t^\beta u(t) \in C((0, T]; L^2(\Omega))$. What is more, Inequality (21) holds.

Since $\dot{H}^2(\Omega) \subset L^2(\Omega) \subset \dot{H}^{-p}(\Omega)$ with $p > 0$, we have $u(\cdot, t) \in C([0, T], \dot{H}^{-p}(\Omega))$.

Next, we only need to prove $\lim_{t \rightarrow 0} \|E(t)u_0 - u_0\|_{L^2(\Omega)} = 0$. In fact, formally there we have

$$\|E(t)u_0 - u_0\|_{L^2(\Omega)}^2 = \sum_{j=1}^{\infty} \left[E_{(1-\beta, 1), 1}^1 \left(\frac{-1}{K} t^{1-\beta}, \frac{-\lambda_j}{K} t \right) + \frac{1}{K} t^{1-\beta} E_{(1-\beta, 1), 2-\beta}^1 \left(\frac{-1}{K} t^{1-\beta}, \frac{-\lambda_j}{K} t \right) - 1 \right]^2 |(u_0, \varphi_j)|^2.$$

By the definition of the bivariate Mittag-Leffler function, we see that $\lim_{t \rightarrow 0^+} \left(E_{(1-\beta, 1), 1}^1 \left(\frac{-1}{K} t^{1-\beta}, \frac{-\lambda_j}{K} t \right) - 1 \right) = 0$. By the boundness of $E_{(1-\beta, 1), 2-\beta}^1 \left(\frac{-1}{K} t^{1-\beta}, \frac{-\lambda_j}{K} t \right)$ with $0 < \beta < 1$, we have $\lim_{t \rightarrow 0} \frac{1}{K} t^{1-\beta} E_{(1-\beta, 1), 2-\beta}^1 \left(\frac{-1}{K} t^{1-\beta}, \frac{-\lambda_j}{K} t \right) = 0$ for all $j \in \mathbb{N}_+$. Therefore, $E_{(1-\beta, 1), 1}^1 \left(\frac{-1}{K} t^{1-\beta}, \frac{-\lambda_j}{K} t \right) + \frac{1}{K} t^{1-\beta} E_{(1-\beta, 1), 2-\beta}^1 \left(\frac{-1}{K} t^{1-\beta}, \frac{-\lambda_j}{K} t \right) - 1 = 0$ as $t \rightarrow 0$ for all $j \in \mathbb{N}_+$. In addition, by Lemma 2.4, for all $t \in [0, T]$, we can deduce that

$$\begin{aligned} & \sum_{j=1}^{\infty} \left| E_{(1-\beta, 1), 1}^1 \left(\frac{-1}{K} t^{1-\beta}, \frac{-\lambda_j}{K} t \right) + \frac{1}{K} t^{1-\beta} E_{(1-\beta, 1), 2-\beta}^1 \left(\frac{-1}{K} t^{1-\beta}, \frac{-\lambda_j}{K} t \right) - 1 \right|^2 |(u_0, \varphi_j)|^2 \\ & \leq 2 \sum_{j=1}^{\infty} \left\{ \left(\frac{C}{1 + \frac{\lambda_j t}{K}} \right)^2 + \left(\frac{C t^{1-\beta}}{1 + \frac{\lambda_j t}{K}} \right)^2 + 1 \right\} |(u_0, \varphi_j)|^2 \leq C \sum_{j=1}^{\infty} C' |(u_0, \varphi_j)|^2 \leq C \|u_0\|_{L^2(\Omega)}^2 < \infty. \end{aligned}$$

Therefore, by applying Lebesgue's dominant convergence theorem, we conclude that $\lim_{t \rightarrow 0} \|E(t)u_0 - u_0\|_{L^2(\Omega)} = 0$. Hence, by Definition 2.7, the function $u(t)$ defined in Eq. (24) is indeed a weak solution to problem (1).

Now we turn to prove the uniqueness. We only have to prove Problem (1) has a unique trivial solution under the conditions $u_0 \equiv 0$ and $f \equiv 0$. Utilizing the variable separation method, for $f \equiv 0$, we have

$$K \frac{d}{dt} u_j(t) + \partial_t^\beta u_j(t) + \lambda_j u_j(t) = 0, \quad \text{almost all } t \in (0, T). \quad (31)$$

Since $u(t) \in L^2(\Omega)$ with $t \in (0, T)$ and $u_0 \equiv 0$, we have $\lim_{t \rightarrow 0} \|u(t)\|_{L^2(\Omega)} = 0$, and $u_j(0) = 0$, $j = 1, 2, \dots$. Further, by the existence and uniqueness of the solution of the ordinary differential equation (31) (see Theorem 3.1 in [38] or Corollary 3.7 in [1]), we can get that $u_j(t) = 0$ ($j = 1, 2, 3, \dots$). Since the characteristic function $\{\varphi_j\}_{j \in \mathbb{N}}$ spans a complete orthogonal system in $L^2(\Omega)$ space, therefore, $u(t) = 0$ in $(0, T) \times \Omega$. Thus the proof of Theorem 2.8(I) is completed.

(b) *Proof of Theorem 2.8 (II).*

For $u_0 \in H_0^1(\Omega)$, $t \in (0, T]$, by Eqs. (25) and (26), there hold

$$\|u(t)\|_{\dot{H}^2(\Omega)} + \left\| \frac{d}{dt} u(t) \right\|_{L^2(\Omega)} \leq C t^{-\frac{1}{2}} \|u_0\|_{\dot{H}^1(\Omega)}, \quad \text{and} \quad \left\| \partial_t^\beta u(t) \right\|_{L^2(\Omega)} \leq c t^{\frac{1}{2}-\beta} \|u_0\|_{\dot{H}^1(\Omega)}.$$

Therefore, $Au(t) \in C((0, T]; L^2(\Omega))$, $\partial_t u(t) \in C((0, T], L^2(\Omega))$ and $\partial_t^\beta u(t) \in C((0, T]; L^2(\Omega))$. Thus $u(t) \in C^1((0, T]; L^2(\Omega)) \cap C((0, T]; H^2(\Omega) \cap H_0^1(\Omega))$. Moreover, by Eq. (25), for any $0 < \varepsilon < 1$, we can deduce that

$$\begin{aligned} \|u(t)\|_{\dot{H}^{2-\varepsilon}(\Omega)}^2 &= \sum_{j=1}^{\infty} \lambda_j^{2-\varepsilon} \left[E_{(1-\beta, 1), 1}^1 \left(\frac{-1}{K} t^{1-\beta}, \frac{-\lambda_j}{K} t \right) + \frac{1}{K} t^{1-\beta} E_{(1-\beta, 1), 2-\beta}^1 \left(\frac{-1}{K} t^{1-\beta}, \frac{-\lambda_j}{K} t \right) \right]^2 |(u_0, \varphi_j)|^2 \\ &\leq C \sum_{j=1}^{\infty} \left[\frac{(\lambda_j t)^{\frac{1}{2}-\frac{\varepsilon}{2}} t^{-\frac{1}{2}+\frac{\varepsilon}{2}}}{K + \lambda_j t} \lambda_j^{\frac{1}{2}} |(u_0, \varphi_j)| \right]^2 + C t^{2(1-\beta)} \sum_{j=1}^{\infty} \left[\frac{(\lambda_j t)^{\frac{1}{2}-\frac{\varepsilon}{2}} t^{-\frac{1}{2}+\frac{\varepsilon}{2}}}{K + \lambda_j t} \lambda_j^{\frac{1}{2}} |(u_0, \varphi_j)| \right]^2 \\ &\leq C t^{-1+\varepsilon} \sum_{j=1}^{\infty} C' \lambda_j |(u_0, \varphi_j)|^2 \leq C t^{-1+\varepsilon} \|u_0\|_{\dot{H}^1(\Omega)}^2. \end{aligned}$$

Since $0 < 1 - \varepsilon < 1$, we have $\|u(t)\|_{L^2(0, T; \dot{H}^{2-\varepsilon})} \leq C \|u_0\|_{\dot{H}^1(\Omega)}$, which implies that $u(t) \in L^2(0, T; H^{2-\varepsilon}(\Omega) \cap H_0^1(\Omega))$. Therefore the proof of Theorem 2.8 (II) is completed.

(c) *Proof of Theorem 2.8 (III).*

Let $u_0 \in H^2(\Omega) \cap H_0^1(\Omega)$. Then for $t \in [0, T]$, by Eq. (25), it is easy to get $\|u(t)\|_{\dot{H}^2(\Omega)} \leq C \|u_0\|_{\dot{H}^2(\Omega)}$. However, we can not obtain any estimation about $\frac{d}{dt}u(t)$ or $\partial_t^\beta u(t)$ by applying Eq. (26) directly, because of the limitation $p - q > 0$ in it. We need to explore the representation of solution in Subsection 2.2. In fact, from Theorem 2.8 (I), we have known that the mild solution $u(t)$ defined in Eq. (12) is indeed a weak solution to Problem (1). Note that $\eta(z)A^{-1}(\eta(z) + A)^{-1} = A^{-1} - (\eta(z) + A)^{-1}$ and $\int_{\Gamma_{\theta, \delta}} e^{zt} z^{m-1} dz = 0$ with $m \geq 1$. Thus, we have

$$\frac{d}{dt}u(t) = \frac{1}{2\pi i} \int_{\Gamma_{\theta, \delta}} e^{zt} \eta(z) A^{-1} (\eta(z) I + A)^{-1} A u_0 dz = -\frac{1}{2\pi i} \int_{\Gamma_{\theta, \delta}} e^{zt} (\eta(z) I + A)^{-1} A u_0 dz.$$

Then by Proposition 2.2, we get

$$\begin{aligned} \left\| \frac{d}{dt}u(t) \right\|_{L^2(\Omega)} &\leq \frac{C}{2\pi} \int_{\Gamma_{\theta, \delta}} e^{|z|t \cos \theta} \|(\eta(z) I + A)^{-1}\|_{L^2(\Omega)} \|A u_0\|_{L^2(\Omega)} |dz| \\ &\leq \frac{C}{2\pi} \int_{\Gamma_{\theta, \delta}} e^{|z|t \cos \theta} |z|^{-1} \|A u_0\|_{L^2(\Omega)} |dz| \leq C \|u_0\|_{\dot{H}^2(\Omega)}. \end{aligned}$$

Therefore we deduce $u(t) \in C^1([0, T]; L^2(\Omega)) \cap C([0, T]; H^2(\Omega) \cap H_0^1(\Omega))$. Since $f \equiv 0$, we can see that $\left\| \partial_t^\beta u(t) \right\|_{L^2(\Omega)} \leq C \|Au(t)\|_{L^2(\Omega)} + C \left\| \frac{d}{dt}u(t) \right\|_{L^2(\Omega)} \leq C \|u_0\|_{\dot{H}^2(\Omega)}$, and $\partial_t^\beta u(t) \in C([0, T]; L^2(\Omega))$. Finally, the estimation in Eq. (23) is obtained. \square

Next, we turn to the inhomogeneous case with vanishing initial value.

Theorem 2.9. *Let $0 < \beta < 1$, $K > 0$ and $u_0 \equiv 0$. If $f \in L^\infty(0, T; L^2(\Omega))$, then $u(t)$ defined in Eq. (18) is the unique weak solution to Problem (1), belonging to $C^1([0, T]; L^2(\Omega)) \cap L^2(0, T; H^2 \cap H_0^1(\Omega))$, $\partial_t^\beta u(t) \in L^2((0, T) \times \Omega)$ with $\partial_t u(t) \in L^2((0, T) \times \Omega)$. In particular, for $p > d/2$ ($d = 1, 2$ or 3 is the spacial dimension), $u(t) \in C([0, T]; \dot{H}^{-p}(\Omega))$, and*

$$\lim_{t \rightarrow 0} \|u(t) - u_0\|_{\dot{H}^{-p}(\Omega)} = 0.$$

Furthermore, there exists a positive constant C such that following estimate holds:

$$\|u(t)\|_{L^2(0, T; \dot{H}^2(\Omega))} + \left\| \frac{\partial}{\partial t}u(t) \right\|_{L^2((0, T) \times \Omega)} + \left\| \partial_t^\beta u(t) \right\|_{L^2((0, T) \times \Omega)} \leq C \|f\|_{L^2((0, T) \times \Omega)}. \quad (32)$$

Proof. If $u_0 \equiv 0$, then according to the expression of $u(t)$ in Eq. (18), we have

$$u(t) = \sum_{j=1}^{\infty} \int_0^t E_{(1-\beta,1),1}^1 \left(\frac{-1}{K}(t-\tau)^{1-\beta}, \frac{-\lambda_j}{K}(t-\tau) \right) (f(\tau), \varphi_j) d\tau \cdot \varphi_j. \quad (33)$$

By Lemma 2.4 and Young's inequality, for any $\nu \in (0, 1)$, there holds

$$\begin{aligned} \|u(t)\|_{\dot{H}^2(\Omega)}^2 &= \sum_{j=1}^{\infty} \lambda_j^2 \left(\int_0^t E_{(1-\beta,1),1}^1 \left(\frac{-1}{K}(t-\tau)^{1-\beta}, \frac{-\lambda_j}{K}(t-\tau) \right) (f(\tau), \varphi_j) d\tau \right)^2 \\ &\leq C \sum_{j=1}^{\infty} \left(\int_0^t \frac{\lambda_j(t-\tau)^\nu (t-\tau)^{-\nu}}{\left(1 + \frac{\lambda_j(t-\tau)}{K}\right)} |(f(\tau), \varphi_j)| d\tau \right)^2 \\ &\leq C \sum_{j=1}^{\infty} \left(\int_0^t (t-\tau)^{-\nu} d\tau \right)^2 \left(\int_0^t |(f(\tau), \varphi_j)|^2 d\tau \right) \\ &\leq C t^{2-2\nu} \int_0^T \|f(t)\|_{L^2(\Omega)}^2 dt \leq C \|f(t)\|_{L^2((0,T)\times\Omega)}^2, \end{aligned} \quad (34)$$

where the second inequality holds because $\sup_{j \in \mathbb{N}} \frac{\lambda_j(t-\tau)^\nu}{1 + \frac{\lambda_j(t-\tau)}{K}} \leq C'$ uniformly for $\nu \in (0, 1)$. Therefore, we deduce that $Au(t) \in C([0, T]; L^2(\Omega))$, which implies $u(t) \in C([0, T]; H^2(\Omega) \cap H_0^1(\Omega))$. Furthermore, we can see that $\|u(t)\|_{L^2(0,T;\dot{H}^2(\Omega))} \leq C \|f\|_{L^2((0,T)\times\Omega)}$, i.e., $u(t) \in L^2(0, T; H^2 \cap H_0^1(\Omega))$.

Next, according to the differential properties of the convolution (i.e., $\partial_t[f_1(t) * f_2(t)] = \partial_t f_1(t) * f_2(t) + f_1(0)f_2(t)$), there holds

$$\begin{aligned} &\frac{d}{dt} \int_0^t E_{(1-\beta,1),1}^1 \left(\frac{-1}{K}(t-\tau)^{1-\beta}, \frac{-\lambda_j}{K}(t-\tau) \right) (f(\tau), \varphi_j) d\tau \\ &= \int_0^t \frac{d}{dt} E_{(1-\beta,1),1}^1 \left(\frac{-1}{K}(t-\tau)^{1-\beta}, \frac{-\lambda_j}{K}(t-\tau) \right) (f(\tau), \varphi_j) d\tau + (f(\tau), \varphi_j). \end{aligned} \quad (35)$$

By the complex contour integral representation of the bivariate Mittag-Leffler function in Eq. (71), we get

$$E_{(1-\beta,1),1}^1 \left(\frac{-1}{K}t^{1-\beta}, \frac{-\lambda_j}{K}t \right) = 1 - \frac{1}{K}t^{1-\beta} E_{(1-\beta,1),2-\beta} \left(\frac{-1}{K}t^{1-\beta}, \frac{-\lambda_j}{K}t \right) - \frac{\lambda_j t}{K} E_{(1-\beta,1),2} \left(\frac{-1}{K}t^{1-\beta}, \frac{-\lambda_j}{K}t \right). \quad (36)$$

Combining Eq. (35) and Eq. (36), with Lemmata 2.4 and 2.5, and Young's inequality, we have

$$\begin{aligned} \left\| \frac{d}{dt} u(t) \right\|_{L^2(\Omega)}^2 &= \sum_{j=1}^{\infty} \left(\frac{d}{dt} \int_0^t E_{(1-\beta,1),1}^1 \left(\frac{-1}{K}(t-\tau)^{1-\beta}, \frac{-\lambda_j}{K}(t-\tau) \right) (f(\tau), \varphi_j) d\tau \right)^2 \\ &\leq \sum_{j=1}^{\infty} \left[\int_0^t \left(\frac{(t-\tau)^{-\beta}}{K} E_{(1-\beta,1),1-\beta}^1 \left(\frac{-1}{K}(t-\tau)^{1-\beta}, \frac{-\lambda_j}{K}(t-\tau) \right) \right. \right. \\ &\quad \left. \left. - \frac{\lambda_j}{K} E_{(1-\beta,1),1}^1 \left(\frac{-1}{K}(t-\tau)^{1-\beta}, \frac{-\lambda_j}{K}(t-\tau) \right) \right) |(f(\tau), \varphi_j)| d\tau \right]^2 + C \sum_{j=1}^{\infty} \int_0^t |(f(\tau), \varphi_j)|^2 d\tau \\ &\leq C \sum_{j=1}^{\infty} \left(\int_0^t \frac{(t-\tau)^{-\beta}}{K + \lambda_j(t-\tau)} d\tau \right)^2 \int_0^t |(f(\tau), \varphi_j)|^2 d\tau \end{aligned}$$

$$\begin{aligned}
& + C \sum_{j=1}^{\infty} \left(\int_0^t \frac{(\lambda_j(t-\tau))^\nu (t-\tau)^{-\nu}}{K + \lambda_j(t-\tau)} d\tau \right)^2 \int_0^t |(f(\tau), \varphi_j)|^2 d\tau + C \sum_{j=1}^{\infty} \int_0^t |(f(\tau), \varphi_j)|^2 d\tau \\
& \leq C (t^{2-2\beta} + t^{2-2\nu} + 1) \|f(t)\|_{L^2((0,T) \times \Omega)} \leq C \|f(t)\|_{L^2((0,T) \times \Omega)},
\end{aligned} \tag{37}$$

where $\sup_{j \in \mathbb{N}} \frac{1}{K + \lambda_j(t-\tau)} \leq C$ and $\sup_{j \in \mathbb{N}} \frac{(\lambda_j(t-\tau))^\nu}{K + \lambda_j(t-\tau)} \leq C$ with $\nu \in (0, 1)$ are used. Thus, $u(t) \in C^1([0, T], L^2(\Omega))$, and we have $\int_0^T \|\partial_t u(t)\|_{L^2(\Omega)}^2 \leq C \|f(t)\|_{L^2((0,T) \times \Omega)}$.

With these analyses, it can be obtained that $u(t) \in C^1([0, T]; L^2(\Omega)) \cap L^2(0, T; H^2(\Omega) \cap H_0^1(\Omega))$ and $\partial_t u(t) \in L^2((0, T) \times \Omega)$.

Furthermore, by means of Laplace transform

$$\mathfrak{L}_t \left\{ \partial_t^\beta \left[E_{(1-\beta, 1), 1}^1 \left(\frac{-1}{K} t^{1-\beta}, \frac{-\lambda_j}{K} t \right) * (f(\tau), \varphi_j) \right], z \right\} = \frac{z^{-(1-\beta)}}{1 + \frac{1}{K} z^{\beta-1} + \frac{\lambda_j}{K} z^{-1}} (\hat{f}(z), \varphi_j),$$

we deduce that

$$\begin{aligned}
& \partial_t^\beta \int_0^t E_{(1-\beta, 1), 1}^1 \left(\frac{-1}{K} (t-\tau)^{1-\beta}, \frac{-\lambda_j}{K} (t-\tau) \right) (f(\tau), \varphi_j) d\tau \\
& = \int_0^t (t-\tau)^{-\beta} E_{(1-\beta, 1), 1-\beta}^1 \left(\frac{-1}{K} (t-\tau)^{1-\beta}, \frac{-\lambda_j}{K} (t-\tau) \right) (f(\tau), \varphi_j) d\tau.
\end{aligned}$$

Further, by Young's inequality, we obtain

$$\begin{aligned}
\|\partial_t^\beta u(t)\|_{L^2(\Omega)}^2 & = \sum_{j=1}^{\infty} \left(\int_0^t (t-\tau)^{-\beta} E_{(1-\beta, 1), 1-\beta}^1 \left(\frac{-1}{K} (t-\tau)^{1-\beta}, \frac{-\lambda_j}{K} (t-\tau) \right) (f(\tau), \varphi_j) d\tau \right)^2 \\
& \leq C \sum_{j=1}^{\infty} \left(\int_0^t \frac{(t-\tau)^{-\beta}}{\left(1 + \frac{\lambda_j(t-\tau)}{K}\right)} |(f(\tau), \varphi_j)| d\tau \right)^2 \\
& \leq C t^{2-2\beta} \sum_{j=1}^{\infty} \int_0^T |(f(\tau), \varphi_j)|^2 dt \leq C \|f(t)\|_{L^2((0,T) \times \Omega)}^2.
\end{aligned} \tag{38}$$

Now we have $\partial_t^\beta u(t) \in L^2((0, T) \times \Omega)$ and $\int_0^T \|\partial_t^\beta u(t)\|_{L^2(\Omega)}^2 \leq C \|f(t)\|_{L^2((0,T) \times \Omega)}^2$. Therefore, we get $\partial_t^\beta u(t) \in L^2((0, T) \times \Omega)$.

Last, according to Definition 2.7, we only have to prove $\lim_{t \rightarrow 0} \|u(\cdot, t)\|_{\dot{H}^{-p}} = 0$. In fact, by Eq. (33), there holds

$$\begin{aligned}
\|u(\cdot, t)\|_{\dot{H}^{-p}}^2 & = \sum_{j=1}^{\infty} \frac{1}{\lambda_j^p} \left(\int_0^t E_{(1-\beta, 1), 1}^1 \left(\frac{-1}{K} (t-\tau)^{1-\beta}, \frac{-\lambda_j}{K} (t-\tau) \right) (f(\tau), \varphi_j) d\tau \right)^2 \\
& \leq \sum_{j=1}^{\infty} \frac{1}{\lambda_j^p} \sup_{0 \leq \tau \leq T} |(f(\tau), \phi_j)|^2 \left| \int_0^t E_{(1-\beta, 1), 1}^1 \left(\frac{-1}{K} (t-\tau)^{1-\beta}, \frac{-\lambda_j}{K} (t-\tau) \right) d\tau \right|^2 \\
& \leq C \|f(t)\|_{L^\infty(0, T; L^2(\Omega))}^2 \sum_{j=1}^{\infty} \frac{1}{\lambda_j^p} \left| \int_0^t E_{(1-\beta, 1), 1}^1 \left(\frac{-1}{K} (t-\tau)^{1-\beta}, \frac{-\lambda_j}{K} (t-\tau) \right) d\tau \right|^2,
\end{aligned}$$

where $\|f(t)\|_{L^\infty(0, T; L^2(\Omega))} := \text{ess sup}_{0 \leq t \leq T} \|f(t)\|_{L^2(\Omega)}$. Since $\lambda_j \geq c j^{2/d}$ with $j \in \mathbb{N}_+$ (cf. [7]), and $p > \frac{d}{2}$, then $\sum_{j=1}^{\infty} \frac{1}{\lambda_j^p}$ is bounded. Also, with the boundness of the function $E_{(1-\beta, 1), 1}^1(\frac{-1}{K}(t-\tau)^{1-\beta}, \frac{-\lambda_j}{K}(t-\tau))$, it follows that

$\sum_{j=1}^{\infty} \frac{1}{\lambda_j^p} |\int_0^t E_{(1-\beta,1),1}^1(\frac{-1}{K}(t-\tau)^{1-\beta}, \frac{-\lambda_j}{K}(t-\tau))d\tau|^2 < \infty$, and $\lim_{t \rightarrow 0} |\int_0^t E_{(1-\beta,1),1}^1(\frac{-1}{K}(t-\tau)^{1-\beta}, \frac{-\lambda_j}{K}(t-\tau))d\tau| = 0$ for each $j \in \mathbb{N}_+$. With these, we know that $u(t) \in C([0, T]; \dot{H}^{-p}(\Omega))$ with $p > d/2$. Also, by Lebesgue's dominant convergence theorem, there holds $\lim_{t \rightarrow 0} \|u(\cdot, t)\|_{\dot{H}^{-p}} = 0$. Therefore, $u(t)$ defined in Eq. (33) is indeed a weak solution to Problem (1) with $u_0 = 0$. The uniqueness is the same as been proved in Theorem 2.8(I). Thus the proof is completed. \square

2.3.2. Comparison of our results with standard diffusion equation and sub-diffusion equation

Comparing with the classical diffusion equation (i.e., $K = 0$ and $\beta = 1$) and the sub-diffusion equation (i.e., $K = 0$ and $0 < \beta < 1$), from the above analyses, the new model (i.e., $K > 0$) discussed in this paper possesses the following interesting features:

- (i): From the view of the physical background of the models, the classical diffusion equation is a macro description of Brownian motion; the sub-diffusion equation reflects that the transport rate of the micro particles is slower than that of Brownian motion; while the model (1) with $K > 0$ depicts a crossover from sub-diffusion diffusion (as $t \rightarrow 0$) to normal diffusion (as $t \rightarrow \infty$). Therefore, the model (1) discussed in this paper can improve and enrich the modeling delicacy in depicting the anomalous diffusion.
- (ii): In terms of the regularity of the solution for $f \equiv 0$, if the initial value $u_0 \in L^2(\Omega)$, then by Eq. (21), we have the same results as for the classical situation ($\|u(t)\|_{\dot{H}^2(\Omega)} \leq Ct^{-1}\|u_0\|_{L^2(\Omega)}$), but it is different from the case of sub-diffusion ($\|u(t)\|_{\dot{H}^2(\Omega)} \leq Ct^{-\beta}\|u_0\|_{L^2(\Omega)}$, cf. [7]), which has weak singularity w.r.t. the initial value.

If the initial value is smooth, i.e., $u_0 \in H^2(\Omega) \cap H_0^1(\Omega)$, then from Theorem 2.8 (III), the solution of the new model (1) satisfies that $u(t) \in C^1([0, T], L^2(\Omega)) \cap C([0, T]; L^2(\Omega)) \cap C([0, T]; H^2(\Omega) \cap H_0^1(\Omega))$, comparing with the corresponding results of the regularity of the sub-diffusion $u(t) \in C([0, T]; L^2(\Omega)) \cap C([0, T]; H^2(\Omega) \cap H_0^1(\Omega))$ and $\partial_t^\beta u(t) \in C([0, T]; L^2(\Omega)) \cap C([0, T]; H_0^1(\Omega))$ (cf. [7, 12, 43]). Therefore, we deduce that the regularity of the solution to Problem (1) with $K > 0$ is indeed improved.

With this, we conclude that the time regularity of the solution to TFDE is dominated by the highest-order operator in it.

- (iii): Eq. (27) shows the decay of the solution to Model (1) is t^{-1} as $t \rightarrow \infty$, which is similar to that of the classical diffusion problem. However, Corollaries 2.6 and 2.7 in [7] show that the decay of solution to the sub-diffusion model is $t^{-\beta}$ as $t \rightarrow \infty$, which is slower than these situations in classical diffusion equation as well as in new model.
- (iv): If $u_0 \equiv 0$, $f \in L^2((0, T) \times \Omega)$, and $\beta = 1$, then the prior estimation for the sub-diffusion equation is (Theorem 2.2, Eq. (2.5) in [7]): $\|u(t)\|_{L^2([0, T]; \dot{H}^2(\Omega))} + \|\partial_t^\beta u(t)\|_{L^2((0, T) \times \Omega)} \leq C\|f\|_{L^2((0, T) \times \Omega)}$, which is consistent with the estimation for the classical diffusion equation, i.e., $\|u(t)\|_{L^2(0, T; \dot{H}^2(\Omega))} + \|\frac{\partial}{\partial t} u(t)\|_{L^2((0, T) \times \Omega)} \leq C\|f\|_{L^2((0, T) \times \Omega)}$ (see Page 382, Theorem 5 in [2]). This fact is also the same with our estimation in Eq. (32) for $\beta = 1$.

3. TIME SEMI-DISCRETIZATION AND ERROR ESTIMATION

In this section, we shall develop CIM for time semi-discretization. Error analysis will also be carried out.

3.1. CIM for Problem (1)

Following the basic ideas of CIM introduced in Sec. 1, an appropriate integral contour must be selected firstly. In this paper, we choose the hyperbolic integral contour (cf. [25, 26]), which is parameterized as

$$\Gamma : z(\phi) = \mu(1 + \sin(i\phi - \alpha)) \quad \text{with } \phi \in S, \quad (39)$$

where $\mu > 0$, $\alpha > 0$ are parameters that need to be determined (see Eq. (48)); S is an open strip (see Figure 1 left), defined as $S := \{\phi = x + iy \in \mathbb{C}, x \in \mathbb{R}, |y| < \tilde{d}\}$, where $\tilde{d} = \min\{\alpha, \pi/2 - \alpha - \delta'\}$ with

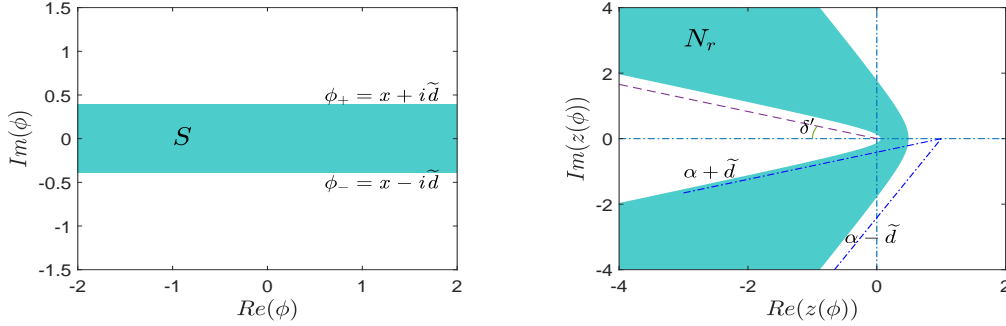


FIGURE 1. A diagram of the symmetrical open strip S (left) and the neighbourhood N_r (right). The parameters are taken as $\alpha = \pi/4$, $\mu = 0.8$ and $\delta' = \pi/8$.

$0 < \alpha - \tilde{d} < \alpha + \tilde{d} < \frac{\pi}{2} - \delta'$ and $\delta' \in (0, \pi/2)$ is the dip angle of asymptote of hyperbola (39). The reason for designing such S is given in the sequence.

Recalling the expression of $z(\phi)$ in Eq. (39), the image of the horizontal line $\phi = x + iy \in S$ is

$$z(x + iy) = \mu(1 - \sin(\alpha + y) \cosh(x)) + i\mu \cos(\alpha + y) \sinh(x),$$

which can be expressed by the hyperbola

$$\left(\frac{\mu - u}{\sin(\alpha + y)} \right)^2 - \left(\frac{v}{\cos(\alpha + y)} \right)^2 = \mu^2 \quad \text{with } z = u + iv.$$

With these, we can see that, for $y > 0$, as y increases from 0 to $\pi/2 - \alpha$, the left branch of this hyperbola $z(\phi)$ will close and degenerate into the negative real axis; for, $y < 0$, when y decreases from 0 to $-\alpha$, $z(\phi)$ will widen and become a vertical line. Since the integral contour we choose cannot degenerate into the real axis (see Remark 2.1), therefore the included angle between the asymptotic line of the hyperbola and the real axis (denotes as δ'), can not be equal to zero. In other words, the upper bound of y is $\pi/2 - \alpha - \delta'$ with $\delta' > 0$, and the width of the strip S satisfies $|y| < \tilde{d}$, with $\tilde{d} = \min\{\alpha, \pi/2 - \alpha - \delta'\}$.

According to the definition of $z(\phi)$, it is clear that $z(\phi)$ is a conformal transformation, which maps the open strip S into a neighbourhood in z -plan (see Fig. 1 (right)), and is denote as $N_r := \{z(\phi) \in \mathbb{C} : \phi \in S\}$. For a fixed $\delta' > 0$, by Remark 2.1 and the definition of $z(\phi)$, there is $N_r \subseteq \Sigma_\theta$. Hence, the integrand $\hat{u}(z)$ is analytic on $z(\phi) \in N_r$, and the integral (12) can be written as

$$u(t) = I := \int_{-\infty}^{+\infty} v(t, r, \phi) d\phi, \quad (40)$$

where

$$v(t, r, \phi) = \frac{1}{2\pi i} e^{z(\phi)t} \hat{u}(z(\phi)) z'(\phi), \quad (41)$$

and $\hat{u}(z)$ is defined in Eq. (11).

Assuming that the Laplace transform of the source term $f(t)$ exists (i.e., $|f(t)| < e^{\sigma_0 t}$), by Riemann-Schwarz reflection principle, there holds $\hat{f}(\bar{z}) = \overline{\hat{f}(z)}$. Since the integral contour Γ defined in Eq. (39) is symmetric w.r.t. the real axis, therefore $\hat{u}(\overline{z(\phi)}) = \overline{\hat{u}(z(\phi))}$. After using the mid-point rule to approximate integral in Eq. (40)

with uniform step-spacing τ , we can obtain CIM for time semi-discretization of Problem (1):

$$u^N(t) = I_{\tau;N} := \tau \sum_{k=1-N}^{N-1} v(t, r, \phi_k) = \frac{\tau}{2\pi i} \sum_{k=1-N}^{N-1} e^{z(\phi_k)t} \hat{u}(z(\phi_k)) z'(\phi_k) = \frac{\tau}{\pi} \text{Im} \left\{ \sum_{k=0}^{N-1} e^{z(\phi_k)t} \hat{u}(z(\phi_k)) z'(\phi_k) \right\}, \quad (42)$$

where $\phi_k = (k + 1/2)\tau$, $k = 0, 1, \dots, N-1$.

3.2. Convergence analysis of CIM scheme (42)

In this subsection, we shall analyze the convergence of scheme (42). For this, we further assume that $f(t) \in L^1(\Omega)$, then $\hat{f}(z)$ might be continued as a analytic function in Σ_θ with fixed $\theta \in (\pi/2, \pi)$. With this, the estimates can be expressed in terms of $\hat{f}(z)$ rather than $f(t)$ (cf. [27]). We also define

$$\|\hat{f}(z)\|_D := \sup_{z \in D} \|\hat{f}(z)\|_{L^2(\Omega)}, \quad D \subseteq \Sigma_\theta. \quad (43)$$

In this paper, we take $D = N_r$.

By introducing the series $I_\tau := \tau \sum_{k=-\infty}^{\infty} v(t, r, \phi_k)$ and $I_{\tau;N;\epsilon} = \tau \sum_{k=1-N}^{N-1} v(t, r, \phi_k)(1 + \epsilon_k)$ (which will be explained in the sequence), the error of CIM scheme (42) can be splitted into

$$E_N := \|u(t) - u^N(t)\|_{L^2(\Omega)} \leq \|I - I_\tau\|_{L^2(\Omega)} + \|I_\tau - I_{\tau;N}\|_{L^2(\Omega)} + \|I_{\tau;N} - I_{\tau;N;\epsilon}\|_{L^2(\Omega)} = DE + TE + RE, \quad (44)$$

where $DE := \|I - I_\tau\|_{L^2(\Omega)}$ is the discretization error, $TE := \|I_\tau - I_{\tau;N}\|_{L^2(\Omega)}$ is the truncation error and $RE := \|I_{\tau;N} - I_{\tau;N;\epsilon}\|_{L^2(\Omega)}$ is usually defined as the round-off error. The reason why we introduce the series $I_{\tau;N;\epsilon}$ is mainly because that $\frac{1}{2\pi i} e^{z(\phi_k)t} \hat{u}(z(\phi_k)) z'(\phi_k)$ is approximated by $\frac{1}{2\pi i} e^{z_k t} \hat{u}_k z'_k$, where $\{\hat{u}_k\}_{k=1-N}^{N-1}$ are provided by means of solving the linear system (60) with prescribed accuracy ϵ . That is, $\|\hat{u}_k - \hat{u}(z(\phi_k))\|_{L^2(\Omega)} < \epsilon_k$, where ϵ_k s are the relative errors in the computed function values $\hat{u}(z(\phi_k))$ and $|\epsilon_k| < \epsilon$ for all $k = \pm 1, \pm 2, \dots, \pm(N-1)$. The evaluations of the elementary functions involved in $v(t, r, \phi_k)$ (such as $\exp(z_k t)$, z'_k and z_k , etc.) turn out to be negligible compared to ϵ (see [26]). Therefore, $\|e^{z_k t} \hat{u}_k z'_k - e^{z(\phi_k)t} \hat{u}(\phi_k) z'(\phi_k)\|_{L^2(\Omega)} \leq \epsilon_k \|e^{z_k t} \hat{u}(z(\phi_k)) z'(\phi_k)\|_{L^2(\Omega)}$ and $I_{\tau;N;\epsilon}$ make sense.

To estimate (47), we need to discuss the properties of the integrand $v(t, r, \phi_k)$.

Firstly, for $z \in N_r \subseteq \Sigma_\theta$ with $|z| > \delta$ (where δ satisfies the condition in Proposition 2.2), by Proposition 2.2, there exists a positive constant C , such that the integrand $\hat{u}(z)$ defined in Eq. (11) satisfies

$$\|\hat{u}(z)\|_{L^2(\Omega)} \leq C|z|^{-1} \left(\|u_0\|_{L^2(\Omega)} + \|\hat{f}(z)\|_{N_r} \right). \quad (45)$$

The following lemma is also needed.

Lemma 3.1 (Lemma 1 in [25]). *Set $L(x) := 1 + |\ln(1 - e^{-x})|$, $x > 0$. There hold*

$$\int_0^{+\infty} e^{-\gamma \cosh(x)} dx \leq L(\gamma), \quad \gamma > 0,$$

and for $\sigma > 0$,

$$\int_\sigma^{+\infty} e^{-\gamma \cosh(x)} dx \leq (1 + L(\gamma))e^{-\gamma \cosh(\sigma)}, \quad \gamma > 0.$$

Obviously, the function $L(x)$ is decreasing with respect to its independent variable x , $L(x) \rightarrow 1$ as $x \rightarrow \infty$ and $L(x) \sim |\ln x|$ as $x \rightarrow 0^+$. Then the integrand $v(t, r, \phi_k)$ has the properties shown in the following proposition.

Proposition 3.2. *Let $v(t, r, \phi)$ be defined in Eq. (41) with $z(\phi) \in N_r \subset \Sigma_\theta$ and $\phi = x \pm iy \in S$. For $t > 0$, if $\|\widehat{f}(z)\|_{N_r} < \infty$ and $u_0 \in L^2(\Omega)$, then there exists a positive constant C , such that*

$$\|v(t, r, \phi)\|_{L^2(\Omega)} \leq C\varphi(\alpha, \tilde{d})e^{\mu t} \left(\|u_0\|_{L^2(\Omega)} + \|\widehat{f}(z)\|_{N_r} \right) e^{-\mu t \sin \alpha \cosh x}, \quad \varphi(\alpha, \tilde{d}) = \sqrt{\frac{1 + \sin(\alpha + \tilde{d})}{1 - \sin(\alpha + \tilde{d})}}. \quad (46)$$

The proof is shown in Appendix B.

Since the integrand $v(t, r, \phi)$ with $\phi = x \pm iy \in S$ has the decay property described in Proposition 3.2, by following the proof of Theorem 2 in [25], we can get the uniform estimates of DE and TE on $t_0 \leq t \leq t_1 = \Lambda t_0$ with $t_0 > 0$ and $\Lambda = t_1/t_0 > 1$:

$$DE + TE \leq C\varphi(\alpha, \tilde{d})L(\mu t_0 \sin(\alpha - \tilde{d})) \left(\|u_0\|_{L^2(\Omega)} + \|\widehat{f}(z)\|_{N_r} \right) e^{\mu t_0 \Lambda} \left(\frac{1}{e^{2\pi \tilde{d}/\tau} - 1} + \frac{1}{e^{\mu t_0 \sin(\alpha - \tilde{d}) \cosh(N\tau)}} \right). \quad (47)$$

Let $\varrho \in (0, 1)$. As the way used in Theorem 1 of [26], when we take

$$\tau = \frac{a(\varrho)}{N}, \quad \text{and} \quad \mu = \frac{2\pi \tilde{d} N(1 - \varrho)}{t_0 \Lambda a(\varrho)}, \quad (48)$$

with $a(\varrho) := \cosh^{-1} \left(\frac{\Lambda}{(1 - \varrho) \sin(\alpha - \tilde{d})} \right)$, the estimate in Eq. (47) can be rewritten as

$$DE + TE \leq C\varphi(\alpha, \tilde{d}) \cdot L(\mu t_0 \sin(\alpha - \tilde{d})) \left(\|u_0\|_{L^2(\Omega)} + \|\widehat{f}(z)\|_{N_r} \right) e^{\mu \Lambda t_0} \frac{2\epsilon_N(\varrho)}{1 - \epsilon_N(\varrho)}, \quad (49)$$

where

$$\epsilon_N(\varrho) := \exp \left(-\frac{2\pi \tilde{d} N}{a(\varrho)} \right). \quad (50)$$

As for RE , since

$$RE = \|I_{\tau; N} - I_{\tau; N; \epsilon}\|_{L^2(\Omega)} \leq \tau \sum_{k=1-N}^{N-1} \|v(t, r, \phi_k)\|_{L^2(\Omega)} |\epsilon_k| \leq 2\epsilon\tau \sum_{k=0}^{N-1} \|v(t, r, \phi_k)\|_{L^2(\Omega)},$$

then by Proposition 3.2 and Lemma 3.1, and taking τ and μ as in (48), for $t_0 \leq t \leq \Lambda t_0$, there holds

$$\begin{aligned} RE &\leq 2C\epsilon e^{\mu \Lambda t_0} \varphi(\alpha, \tilde{d}) \left(\|u_0\|_{L^2(\Omega)} + \|\widehat{f}(z)\|_{N_r} \right) \tau \sum_{k=0}^{N-1} e^{-\mu t_0 \sin(\alpha - \tilde{d}) \cosh(k+1/2)\tau} \\ &\leq CL(\mu t_0 \sin(\alpha - \tilde{d})) \varphi(\alpha, \tilde{d}) \left(\|u_0\|_{L^2(\Omega)} + \|\widehat{f}(z)\|_{N_r} \right) \epsilon e^{\mu \Lambda t_0}. \end{aligned} \quad (51)$$

Note (cf. [26]) that

$$e^{\mu \Lambda t_0} \epsilon_N(\varrho) = (\epsilon_N(\varrho))^{\varrho-1} \cdot \epsilon_N(\varrho) = (\epsilon_N(\varrho))^{\varrho}. \quad (52)$$

Together with the estimates in (49) and (51), we finally get the error estimation E_N for CIM scheme (42).

Theorem 3.3. *Let $u(t)$ be the solutions to Problem (1), and $u^N(t)$ be given by Eq. (42), respectively. Given Λ and α, δ' with $0 < \alpha, \delta' < \pi/2$. For $t_0 \leq t \leq \Lambda t_0$ and $0 < \varrho < 1$, if $\|\widehat{f}(z)\|_{N_r} < \infty$, and τ, μ are determined in*

Eq. (48), then there uniformly holds

$$\|u(t) - u^N(t)\|_{L^2(\Omega)} \leq CL \left(\mu t_0 \sin(\alpha - \tilde{d}) \right) \varphi(\alpha, \tilde{d}) \left(\|u_0\|_{L^2(\Omega)} + \|\hat{f}(z)\|_{N_r} \right) \left(\epsilon \cdot (\epsilon_N(\varrho))^{e-1} + \frac{(\epsilon_N(\varrho))^e}{1 - \epsilon_N(\varrho)} \right),$$

where $0 < \tilde{d} < \min\{\alpha, \pi/2 - \alpha - \delta'\}$.

For fixed α , Λ and δ' , the optimal free parameter ϱ^* is determined by minimizing the convex function

$$\epsilon \cdot (\epsilon_N(\varrho))^{e-1} + \frac{(\epsilon_N(\varrho))^e}{1 - \epsilon_N(\varrho)}.$$

Then the optimization parameters μ^* and τ^* are determined by submitting ϱ^* into Eq. (48). From these, we can obtain the convergence order of CIM as follows.

Theorem 3.4. *According to Theorem 3.3, for given Λ , and α, δ' with $0 < \alpha, \delta' < \pi/2$ and $0 < \tilde{d} < \min\{\alpha, \pi/2 - \alpha - \delta'\}$, by choosing the parameters provided in Eq. (48) as the optimal parameters of the hyperbolic contour Γ , we get for the actual error*

$$E_N = \mathcal{O}(\epsilon + e^{-CN}) \quad \text{with } C = \mathcal{O}\left(\frac{1}{\ln(\Lambda)}\right).$$

Proof. Based on the previous error analysis, we have $E_N = \mathcal{O}(e^{\mu t_0 \Lambda} \epsilon + e^{\mu t_0 \Lambda - 2\pi \tilde{d}/\tau})$. For the optimal parameters determined in Eq. (48), there holds $C := \mu t_0 \Lambda - 2\pi \tilde{d}/\tau = -\frac{2\pi \tilde{d} N \varrho}{a(\varrho)}$ and $a(\varrho) > \cosh^{-1}(\Lambda) \sim \ln(\Lambda)$ with $\Lambda > 1$. Therefore, $C = \mathcal{O}\left(\frac{1}{\ln(\Lambda)}\right)$. As for $e^{\mu t_0 \Lambda} \epsilon$, because $t_1 = t_0 \Lambda$ is a given (finite) number and $\mu > 0$ is also finite for given N and Λ , so we have $e^{\mu t_0 \Lambda} \epsilon = \mathcal{O}(\epsilon)$. \square

Numerical results in Fig. 3 (right) and Fig. 4 (b) in the sequence (where $\epsilon = 2.22 \times 10^{-16}$ is chosen as the machine precision in IEEE arithmetic) demonstrate that the convergence order $C = \mathcal{O}\left(\frac{1}{\ln(\Lambda)}\right)$ in Theorem 3.4 is indeed optimal. That is, the CIM has spectral accuracy w.r.t. N .

4. SPATIAL SEMI-DISCRETIZATION AND ERROR ESTIMATION

In this section, we develop the spatial semi-discrete scheme by using the standard Galerkin finite element method, and give error estimates for the semi-discrete scheme of space with both smooth and non-smooth initial values, respectively.

4.1. Semi-discrete Galerkin scheme

Let $\mathcal{T}_h = \{\tau_j\}_{j=1}^M$ belong to a family of quasi-uniform triangulations of Ω , with $h = \max_{0 \leq j \leq M} \text{diam}(\tau_j)$, where the boundary triangles are allowed to have one curved edge along $\partial\Omega$, and let S_h denote the piecewise continuous functions on the closure $\overline{\Omega}$ of Ω which reduce to polynomials of degree $\leq r-1$ on each triangle τ_j and vanish outside Ω_h , namely,

$$S_h = \{\chi \in H_0^1(\Omega) \cap C(\overline{\Omega}) ; \chi|_{\tau_j} \in \Pi_{r-1}\},$$

where Π_s denotes the set of polynomials of degree at most s . Then the L^2 -orthogonal projection $P_h : L^2(\Omega) \rightarrow S_h$ can be defined as

$$(P_h u, v_h) = (u, v_h) \quad \forall v_h \in S_h, u \in L^2(\Omega),$$

and the standard Ritz projection $R_h : H_0^1(\Omega) \rightarrow S_h$ is defined as

$$(\nabla R_h u, \nabla v_h) = (\nabla u, \nabla v_h) \quad \forall v_h \in S_h, u \in H_0^1(\Omega).$$

It is well known that the projections P_h and R_h meet the following estimates (see [34], etc.), respectively,

$$\begin{aligned} \|P_h v - v\|_{L^2(\Omega)} + h \|\nabla(P_h v - v)\|_{L^2(\Omega)} &\leq Ch^q \|v\|_{\dot{H}^q(\Omega)} \text{ for all } v \in \dot{H}^q(\Omega), \quad q = 1, 2, \\ \|R_h v - v\|_{L^2(\Omega)} + h \|\nabla(P_h v - v)\|_{L^2(\Omega)} &\leq Ch^q \|v\|_{\dot{H}^q(\Omega)} \text{ for all } v \in \dot{H}^q(\Omega), \quad q = 1, 2. \end{aligned} \quad (53)$$

Besides, P_h satisfies the stability estimate $\|P_h v\|_{L^2(\Omega)} \leq C \|v\|_{L^2(\Omega)}$ for $v \in L^2(\Omega)$.

Based on above, the spatially semi-discrete Galerkin FEM scheme for Problem (1) can be formally described as: for $t > 0$, find $u_h(t) \in S_h$, such that

$$\left(K \frac{\partial u_h(t)}{\partial t}, v_h \right) + \left(\partial_t^\beta u_h(t), v_h \right) + (A u_h(t), v_h) = (f, v_h) \quad \forall v_h \in S_h \quad (54)$$

with the initial value $u_h(0) = u_{0,h}$. The choice of $u_{0,h}$ depends on the smoothness of the initial data u_0 , i.e., we take $u_{0,h} = R_h u_0$ for $u_0 \in H_0^1(\Omega) \cap H^2(\Omega)$, and take $u_{0,h} = P_h u_0$ when $u_0 \in L^2(\Omega)$. In addition, by introducing the finite element version of the operator A as $A_h : S_h \rightarrow S_h$ with

$$(A_h u_h(t), v_h) = (\nabla u_h(t), \nabla v_h) \quad \forall u_h(t), v_h \in S_h,$$

then Eq. (54) turns to:

$$K \frac{\partial u_h(t)}{\partial t} + \partial_t^\beta u_h(t) + A_h u_h = f_h \quad \forall t > 0 \quad (55)$$

in the weak sense, with $f_h(t) = P_h f(t)$. After taking Laplace transform on both sides of Eq. (55), there holds

$$((Kz + z^\beta)I + A_h) \hat{u}_h(z) = (K + z^{\beta-1}) u_{0,h} + \hat{f}_h(z). \quad (56)$$

Transforming the above equation by the inverse Laplace, and denote $W_h(z) := \frac{\eta(z)}{z}(\eta(z)I + A_h)^{-1}$, we have

$$u_h(t) = \frac{1}{2\pi i} \int_{\Gamma_{\theta,\delta}} e^{zt} \left(W_h(z) u_{0,h} + z \eta^{-1}(z) W_h(z) \hat{f}_h(z) \right) dz, \quad (57)$$

where $W_h(z)$ satisfies the following estimates by analogy with Proposition 2.2 (II).

Corollary 4.1. *Let δ satisfy the condition in the statement of Proposition 2.2. For all $z \in \Sigma_{\theta,\delta}$, there hold*

$$\|W_h(z)\|_{L^2(\Omega)} \leq C |z|^{-1}, \quad \|A_h W_h(z)\|_{L^2(\Omega)} \leq C. \quad (58)$$

4.2. The spatial error estimation

In this subsection, we shall perform the error estimation of scheme (55). For the homogeneous case, the spatial error estimation in L^2 -norm with both smooth and non-smooth initial values are shown as follows.

Theorem 4.2. *Let $u(t)$ be the solution to Problem (1) and $u_h(t)$ be given in Eq. (57), respectively. If $f \equiv 0$, then for $0 < t \leq T$, the following error estimations hold:*

(I): Assume $u_0 \in L^2(\Omega)$. Take $u_{0,h} = P_h u_0$. There holds

$$\|u_h(t) - u(t)\|_{L^2(\Omega)} \leq C t^{-1} h^2 \|u_0\|_{L^2(\Omega)}.$$

(II): If $u_0 \in H_0^1(\Omega) \cap H^2(\Omega)$, and $u_{0,h} = R_h u_0$, then there exists a positive constant C such that

$$\|u_h(t) - u(t)\|_{L^2(\Omega)} \leq C h^2 \|u_0\|_{\dot{H}^2(\Omega)}.$$

Proof. Let $f \equiv 0$. For $t > 0$ and $u_{0,h} = P_h u_0$, the error $e(t) := u(t) - u_h(t)$ is given by

$$e(t) = \frac{1}{2\pi i} \int_{\Gamma_{\theta,\delta}} e^{zt} (W_h(z) - W(z)) u_0 dz = \frac{1}{2\pi i} \int_{\Gamma_{\theta,\delta}} e^{zt} \frac{\eta(z)}{z} ((\eta(z)I + A_h)^{-1} P_h - (\eta(z)I + A)^{-1}) u_0 dz.$$

Denote $H := (\eta(z)I + A_h)^{-1} P_h - (\eta(z)I + A)^{-1}$. It can be rewritten as

$$H = P_h ((\eta(z)I + A_h)^{-1} - (\eta(z)I + A)^{-1}) P_h - (I - P_h)(\eta(z)I + A)^{-1} P_h - (\eta(z)I + A)^{-1} (I - P_h).$$

Note that $A(\eta(z)I + A)^{-1} = I - \eta(z)(\eta(z)I + A)^{-1}$ is uniformly bounded for $z \in \Sigma_{\theta,\delta}$, which also holds with A replaced by A_h . With this, according to the proof of Theorem 2.1 in [18], the operator H is uniformly bounded for $z \in \Sigma_{\theta,\delta}$, and further we have $\|H u_0\|_{L^2(\Omega)} \leq C h^2 \|u_0\|_{L^2(\Omega)}$. Therefore, we obtain

$$\|e(t)\|_{L^2(\Omega)} \leq C h^2 \int_{\Gamma_{\theta,\delta}} e^{|z|t \cos \theta} |dz| \|u_0\|_{L^2(\Omega)} \leq C t^{-1} h^2 \|u_0\|_{L^2(\Omega)}.$$

Thus, the proof of Theorem 4.2 (I) is completed.

Let $u_0 \in H_0^1(\Omega) \cap H^2(\Omega)$, $u_{0,h} = R_h u_0$ and $f \equiv 0$. Similar to the analysis above, the error $\tilde{e}(t) := u(t) - u_h(t)$ is given by

$$\tilde{e}(t) = \frac{1}{2\pi i} \int_{\Gamma_{\theta,\delta}} e^{zt} (W_h(z) R_h - W(z)) u_0 dz = \frac{1}{2\pi i} \int_{\Gamma_{\theta,\delta}} e^{zt} \frac{\eta(z)}{z} ((\eta(z)I + A_h)^{-1} R_h - (\eta(z)I + A)^{-1}) u_0 dz.$$

Since $\eta(z)(\eta(z)I + A)^{-1} = I - (\eta(z)I + A)^{-1} A$, which also holds with A replaced by A_h , then we have

$$\tilde{e}(t) = \frac{1}{2\pi i} \int_{\Gamma_{\theta,\delta}} e^{zt} z^{-1} (R_h - I) u_0 dz - \frac{1}{2\pi i} \int_{\Gamma_{\theta,\delta}} e^{zt} z^{-1} ((\eta(z)I + A_h)^{-1} A_h R_h - (\eta(z)I + A)^{-1} A) u_0 dz.$$

Because $A_h R_h = P_h A$, there is $((\eta(z)I + A_h)^{-1} A_h R_h - (\eta(z)I + A)^{-1} A) u_0 = H A u_0$. Further, by the boundness of H and the estimate in Eq. (53), there holds

$$\|\tilde{e}(t)\|_{L^2(\Omega)} \leq C h^2 \int_{\Gamma_{\theta,\delta}} e^{|z|t \cos \theta} |z|^{-1} |dz| \|A u_0\|_{L^2(\Omega)} \leq C h^2 \|u_0\|_{\dot{H}^2(\Omega)}.$$

Then, we finish the proof of Theorem 4.2. □

Next, we turn to the inhomogeneous case with vanishing initial data.

Theorem 4.3. *Let $u(t)$ be the solution to Problem (1) and $u_h(t)$ be given in Eq. (57), respectively. If $u_0 \equiv 0$, and $\|\hat{f}(z)\|_{N_r} < \infty$, then for $0 < t \leq T$, there holds*

$$\|u(t) - u_h(t)\|_{L^2(\Omega)} \leq C h^2 t^{-1} \|\hat{f}(z)\|_{N_r}.$$

Proof. Since $u_0 \equiv 0$, the error $\bar{e}(t) := u_h(t) - u(t)$ is

$$\bar{e}(t) = \frac{1}{2\pi i} \int_{\Gamma_{\theta,\delta}} e^{zt} z \eta(z)^{-1} (W_h(z) P_h - W(z)) \hat{f}(z) dz = \frac{1}{2\pi i} \int_{\Gamma_{\theta,\delta}} e^{zt} ((\eta(z)I + A_h)^{-1} P_h - (\eta(z)I + A)^{-1}) \hat{f}(z) dz.$$

According to the proof of Theorem 4.2 (I), it follows that

$$\|\bar{e}(t)\|_{L^2(\Omega)} \leq C h^2 \int_{\Gamma_{\theta,\delta}} e^{t|z| \cos \theta} \|\hat{f}(z)\|_{N_r} |dz| \leq C h^2 t^{-1} \|\hat{f}(z)\|_{N_r}.$$

□

5. FULL DISCRETE SCHEME AND CONVERGENCE ANALYSIS

The full discrete scheme of Problem (1) can be obtained by applying CIM scheme to Eq. (57), which is given by

$$u_h^N(t) = I_{\tau;h;N} := \tau \sum_{k=1-N}^{N-1} v_h(t, r, \phi_k) = \frac{\tau}{\pi} \text{Im} \left\{ \sum_{k=0}^{N-1} e^{z_k t} \widehat{u}_h(z_k) z'_k \right\}, \quad (59)$$

where $\widehat{u}_h(z_k)$ is obtained by solving Eq. (56) with $z = z_k$, $k = 0, 1, 2, \dots, N-1$. We can see that in order to get the numerical solution $u_h^N(t)$ for a range values of time t , one has to firstly solve N discrete elliptic systems:

$$\left((K z_k + z_k^\beta) \widehat{u}_h(z_k), v_h \right) + (\nabla \widehat{u}_h(z_k), \nabla v_h) = \left((K + z_k^{\beta-1}) u_0 + \widehat{f}(z_k), v_h \right) \quad \forall v_h \in S_h, k = 0, 1, 2, \dots, N-1. \quad (60)$$

It is clear that the main computation of the full discrete scheme (59) is to solve the linear systems (60). Moreover, all of the systems in (60) are tri-diagonal linear algebraic equations with the coefficient matrix being strictly diagonally dominant. Hence, they have unique solutions.

In addition, by combining Theorem 3.3 and Theorem 4.2, we can directly get the following error estimation for the fully discrete scheme (59) with $f \equiv 0$.

Theorem 5.1. *Let $u(t)$ be the solution to Problem (1) and $u_h^N(t)$ be given by Eq. (59), respectively. For $t_0 \leq t \leq \Lambda t_0$, $0 < \varrho < 1$, if $u_0 \in L^2(\Omega)$, there holds*

$$\|u(t) - u_h^N(t)\|_{L^2(\Omega)} \leq C \left(t^{-1} h^2 + L(\mu t_0 \sin(\alpha - \widetilde{d})) \sqrt{\frac{1 + \sin(\alpha + \widetilde{d})}{1 - \sin(\alpha + \widetilde{d})}} \left(\epsilon \cdot (\epsilon_N(\varrho))^{q-1} + \frac{(\epsilon_N(\varrho))^q}{1 - \epsilon_N(\varrho)} \right) \right) \|u_0\|_{L^2(\Omega)}.$$

If $u_0 \in H^2(\Omega) \cap H_0^1(\Omega)$, we have

$$\|u(t) - u_h^N(t)\|_{L^2(\Omega)} \leq C \left(h^2 + L(\mu t_0 \sin(\alpha - \widetilde{d})) \sqrt{\frac{1 + \sin(\alpha + \widetilde{d})}{1 - \sin(\alpha + \widetilde{d})}} \left(\epsilon \cdot (\epsilon_N(\varrho))^{q-1} + \frac{(\epsilon_N(\varrho))^q}{1 - \epsilon_N(\varrho)} \right) \right) \|u_0\|_{H^2(\Omega)}.$$

The parameters selected in the above estimates are $0 < \alpha, \delta' < \pi/2$ and $0 < \widetilde{d} < \min\{\alpha, \pi/2 - \alpha - \delta'\}$.

Also, by combining Theorem 3.3 and Theorem 4.3, we can get the error estimation of the fully discrete scheme for the inhomogeneous problem with vanishing initial data, which is shown in the following theorem.

Theorem 5.2. *Let $u(t)$ be the solution to Problem (1) and $u_h^N(t)$ be given in Eq. (59), respectively. Given Λ , and α, δ' with $0 < \alpha, \delta' < \pi/2$, and $0 < \widetilde{d} < \min\{\alpha, \pi/2 - \alpha - \delta'\}$, then for $t_0 < t < \Lambda t_0$, $0 < \varrho < 1$ and $0 < \gamma < 1$, if $\|\widehat{f}(z)\|_{N_r} < \infty$, there holds*

$$\|u(t) - u_h^N(t)\|_{L^2(\Omega)} \leq C \left(t^{-1} h^2 + L(\mu t_0 \sin(\alpha - \widetilde{d})) \sqrt{\frac{1 + \sin(\alpha + \widetilde{d})}{1 - \sin(\alpha + \widetilde{d})}} \left(\epsilon \cdot (\epsilon_N(\varrho))^{q-1} + \frac{(\epsilon_N(\varrho))^q}{1 - \epsilon_N(\varrho)} \right) \right) \|\widehat{f}(z)\|_{N_r}.$$

6. IMPLEMENTATION AND ACCELERATION OF THE ALGORITHM

To compute one single linear elliptic system in (60), our implementation process is as follows: for 1-D problem, the linear system is solved by Tomas algorithm, which has a computational complexity of $\mathcal{O}(M)$ (So that after combing with CIM algorithm for time discretization, the total computation amount for the solution to Problem

(1) is $\mathcal{O}(MN)$); for 2-D case, we directly employ the command *mldivide*(\cdot, \cdot) in MATLAB to solve the systems (60).

In the sequence, we target on developing an acceleration algorithm for the full discrete scheme (59).

It is clear that, given a contour line $z(\phi)$, to obtain the numerical solution from (59), the main calculation comes from getting $\{\hat{u}_h(z_k)\}_{k=0}^{N-1}$ by solving N elliptic equations in (60). The computational cost will naturally be reduced a lot if we cut down the number of the elliptic systems. Then the question is, how to keep the accuracy of the algorithm at the same time? The answer is that, since $\{\hat{u}_h(z_k)\}_{k=0}^{N-1}$ used in (59) are mutually independent, they can be approximately interpolated by the reduced numbers of solutions of the elliptic systems in (60) on some suitable points chosen from the contour line $z(\phi)$. To avoid Runge phenomenon, we choose n Chebyshev points as the corresponding interpolation nodes on the straight line ϕ .

In numerical implementation, the specific contour $z(\phi)$ we select is the one whose original image be just the real axis $\phi^0 := x + iy, x \in \mathbb{R}, y = 0$. As a matter of fact, by symmetry, we only need to discuss the details on half of $z(\phi^0)$ or ϕ^0 (see Section 3 or (59)).

Denote n Chebyshev points on the standard interval $[-1, 1]$ as $\zeta_j = \cos(\frac{j\pi}{n}), j = 0, 1, 2, \dots, n$, and $n < N$. So the corresponding Chebyshev interpolation nodes used are $z(x_j) := z(\frac{a+b}{2} + \frac{b-a}{2}\zeta_j)$, $j = 0, 1, 2, \dots, n$ with $a = \frac{\tau}{2}, b = ((N-1) + \frac{1}{2})\tau$. We also denote the function values obtained by solving Eq. (60) on the interpolation nodes $z(x_j)$ as $\hat{u}_h(z_{x_j}), k = 0, 1, 2, \dots, n$.

With this, we select the barycentric Lagrange interpolation to approximate all $\{\hat{u}_h(z_k)\}_{k=0}^{N-1}$. (The barycentric interpolation is a variant of Lagrange polynomial interpolation with $\mathcal{O}(n)$ flops, which is fast and stable (see [33] for details).) That is

$$\hat{u}(z_k) \approx \hat{u}_{I,h}(z_k) := \frac{\sum_{j=0}^n \frac{\omega_j}{z_k - z_{x_j}} \hat{u}_h(z_{x_j})}{\sum_{j=0}^n \frac{\omega_j}{z_k - z_{x_j}}}, \quad \omega_j = \frac{1}{\prod_{k \neq m_j} (z_{x_j} - z_k)}, \quad j = 0, 1, \dots, n, \quad (61)$$

where the barycentric weights ω_j are given as (see [33] and the references therein)

$$\omega_j = (-1)^{-j} \delta_j \quad \text{with} \quad \delta_j = \begin{cases} 1/2, & j = 0 \text{ or } j = n, \\ 1, & \text{otherwise.} \end{cases}$$

Until now, the full discrete scheme (59) can be approximately replaced by

$$u_{I,h}^N(t) := \tau \sum_{k=1-N}^{N-1} v_{I,h}(t, \phi_k) = \frac{\tau}{\pi} \text{Im} \left\{ \sum_{k=0}^{N-1} e^{z_k t} \hat{u}_{I,h}(z_k) z_k' \right\}. \quad (62)$$

Combined with the spatial Galerkin FEM, the above process is shown in Algorithm 1 with $\mathcal{O}(n(N+M))$ flops, which we name as ‘‘CIM-Int-FEM’’. In comparison, we also name the corresponding algorithm without acceleration as ‘‘CIM-FEM’’.

Denote $\phi_N^+ := [\frac{\tau}{2}, ((N-1) + \frac{1}{2})\tau]$. We directly employ the result given in [33] on the standard interval $[-1, 1]$ to explain the efficiency of our acceleration algorithm. Firstly, we transform the interpolation from the complex plane that $z(\phi)$ lies in to the standard interval $[-1, 1]$. Denote $\tilde{u}(\zeta) := \hat{u}^N(z)$, $\tilde{u}_{I,h}(\zeta) := \hat{u}_{I,h}^N(z)$, $\zeta \in [-1, 1]$, where $\hat{u}^N(z)$ and $\hat{u}_{I,h}^N(z)$ are the truncation of functions $\hat{u}(z)$ and $\hat{u}_{I,h}(z)$ on $z(\phi_N^+)$, respectively. Then by the discussion in Section 6 of [33], the remainder term $R_n(z) := \hat{u}(z) - \hat{u}_{I,h}(z)$ satisfies the following estimation:

$$\max_{z \in \phi_N^+} |R_n(z)| = \max_{z \in \phi_N^+} |\hat{u}^N(z) - \hat{u}_{I,h}^N(z)| = \max_{\zeta \in [-1, 1]} |\tilde{u}(\zeta) - \tilde{u}_{I,h}(\zeta)| \leq CK^{-n}, \quad (63)$$

where $K > 1$ is a constant, determined by the continued analyticity of \tilde{u} in the complex plane (see Page 174 in [46] for more details). To be precise, if $\tilde{u}(\zeta)$ can be analytically continued to a function \tilde{u} in a complex region around $[-1, 1]$ that includes an ellipse with foci ± 1 and axis lengths $2L$ and $2l$, then we may take $K = L + l$

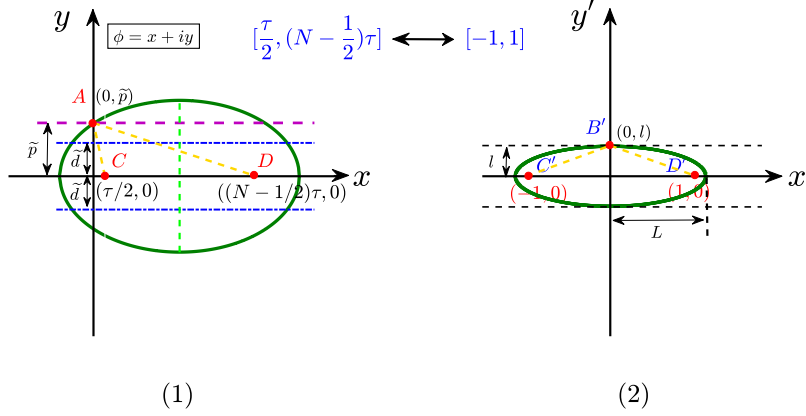


FIGURE 2. Schematic diagram of the maximal elliptic analytic region and its degradation to an elliptic region with focus ± 1 , where $A : (0, \frac{\pi}{2} - \alpha - \varepsilon)$, $C : (\frac{\tau}{2}, 0)$, $D : ((N - \frac{1}{2})\tau, 0)$, $B' : (0, l)$, $C' : (-1, 0)$, $D' : (1, 0)$.

(see Chapter 5 in [47] or Section 6 in [33]). In the sequence, we shall demonstrate the exact values of L and l taken in our situation.

In fact, we only need to fix the biggest corresponding ellipse in the complex plane that ϕ_N^+ lies in. As we have discussed in Subsection 3.1, $\hat{u}(z(\phi_N^+))$ can be analytically continued to $\hat{u}(z(\phi))$ in the ϕ -complex plane until $z(\phi) = 0$ or $\phi = i \cdot (\frac{\pi}{2} - \alpha + 2m\pi)$, $m \in \mathbb{Z}$. So the biggest ellipse, on and inside which \hat{u} is analytic, with foci $C = (\frac{\tau}{2}, 0)$ and $D = ((N - \frac{1}{2})\tau, 0)$ is shown in Fig. 2 (left).

Denote $\tilde{p} := \frac{\pi}{2} - \alpha - \varepsilon$ with a sufficiently small $\varepsilon > 0$. After simple computation, we can see that the equation of this biggest ellipse is

$$\frac{4(x - \frac{N\tau}{2})^2}{\left(\sqrt{\frac{\tau^2}{4} + \tilde{p}^2} + \sqrt{(N - \frac{1}{2})^2\tau^2 + \tilde{p}^2}\right)^2} + \frac{4y^2}{\left(\sqrt{\frac{\tau^2}{4} + \tilde{p}^2} + \sqrt{(N - \frac{1}{2})^2\tau^2 + \tilde{p}^2}\right)^2 - (N - 1)^2\tau^2} = 1.$$

By rescaling, we can get the axis lengths of the correspondingly biggest ellipse on and inside which \tilde{u} is analytic:

$L = \sqrt{(1 + \frac{1}{2(N-1)})^2 + \frac{\tilde{p}^2}{(N-1)^2}\tau^2} + \sqrt{\frac{1}{4(N-1)^2} + \frac{\tilde{p}^2}{(N-1)^2\tau^2}} > 1$, and $l = \sqrt{L^2 - 1}$. Thus,

$$K = L + l = L + \sqrt{L^2 - 1}. \quad (64)$$

Since $K > 1$, we can see from (63) that the rate of the convergence of the interpolants to $\hat{u}(z)$ as $n \rightarrow \infty$ is remarkably fast.

What is more, to estimate the error caused by the above acceleration process in experiments, we will use the following interpolation approximation rate (IAR):

$$IAR = \frac{\|u(t) - u_{I,h}^N(t)\|_{L^2(\Omega)}}{\|u(t)\|_{L^2(\Omega)}}, \quad (65)$$

to verify the effectiveness of our accelerated numerical scheme in the next section, where $u(t)$ is the analytic solution.

Algorithm 1 CIM-Int-FEM**Input:** $\beta; t_0; t_1 = \Lambda t_0; t; \Lambda > 1; \alpha; \delta'; \epsilon; N; M; D$.**Output:** the numerical result $u_{I,h}^N(t)$.

```

1: Subroutine 1: Compute the optimal parameters  $\varrho^*$ ,  $\tau^*$  and  $\mu^*$ .
2: for  $j = 0; j < D; j++$  do
3:    $\varrho_j \leftarrow 1/D \cdot j$ ;
4:    $a(\varrho_j) \leftarrow \cosh^{-1} \left( \frac{\Lambda}{(1-\varrho_j) \sin(\alpha-d)} \right)$ ;
5:    $\epsilon_N(\varrho_j) \leftarrow \exp(\frac{2\pi d N}{a(\varrho_j)})$ ;
6:    $\varrho^* \leftarrow \min_j \left( \epsilon(\epsilon_N(\varrho_j))^{\varrho_j-1} + \frac{(\epsilon_N(\varrho_j))^{\varrho_j}}{1-\epsilon_N(\varrho_j)} \right)$ ;
7: end do
8:    $\tau^*, \mu^* \leftarrow$  Substitute  $\varrho^*$  into Eq. (48) to get the optimal parameters  $\tau^*$  and  $\mu^*$ ;
9: Subroutine 2: Compute the interpolation functions  $\{\hat{u}_h(z_{x_j})\}_{j=0}^{n-1}$  on the Chebyshev points  $\{z(x_j)\}_{j=0}^{n-1}$ .
10: for  $j = 0; j < n; j++$  do
11:    $x_j \leftarrow \frac{a+b}{2} + \frac{b-a}{2} \cos(\frac{j\pi}{n})$  with  $a = \frac{\tau^*}{2}$  and  $b = (N - \frac{1}{2})\tau^*$ ;
12:    $z_{x_j} \leftarrow \mu^*(1 + \sin(ix_j - \alpha))$ , where  $i^2 = -1$ ;
13:    $\hat{u}_h(z_{x_j}) \leftarrow$  Solve  $\left( (Kz_{x_j} + z_{x_j}^\beta) \hat{u}_h(z_{x_j}), v_h \right) + (\nabla \hat{u}_h(z_{x_j}), \nabla v_h) = \left( (K + z_{x_j}^{\beta-1}) u_0 + \hat{f}(z_{x_j}), v_h \right)$ ;
14: end do
15: Subroutine 3: Compute the numerical solution  $u_{I,h}^N(t)$ .
16: for  $k = 0; j < N - 1; k++$  do
17:    $z_k \leftarrow \mu^*(1 + \sin(i(k + 1/2)\tau^* - \alpha))$ , where  $i^2 = -1$ ;
18:    $z'_k \leftarrow i\mu^* \cos(i(k + 1/2)\tau^* - \alpha)$ , where  $i^2 = -1$ ;
19:    $\hat{u}_{I,h}(z_k) \leftarrow \frac{\sum_{j=0}^n \frac{\omega_j}{z_k - z_{x_j}} \hat{u}_h(z_{x_j})}{\sum_{j=0}^n \frac{\omega_j}{z_k - z_{x_j}}}$ ;
20: end do
21:    $u_{I,h}^N(t) \leftarrow \frac{\tau^*}{\pi} \text{Im} \left\{ \sum_{k=0}^{N-1} e^{z_k t} \hat{u}_{I,h}(z_k) z'_k \right\}$ ;

```

7. NUMERICAL EXPERIMENTS

In this section, numerical performances of our developed numerical scheme are given. During the experiments, we always take $\Omega = (0, 1)^d$ with $d = 1, 2$, $T = 1$, $K = 1$, $\alpha = 0.6767$, $\delta' = 0.1023$, and $\epsilon = 2.22 \times 10^{-16}$. For the spacial finite element discretization, the degree of polynomial Π_{r-1} is taken as $r = 2$.

If the exact solution $u(t)$ is known, we define $Error_\tau(N)$ to measure the temporal errors if h is given, and $Error_h(t)$ to measure the spatial errors at time t if N is fixed:

$$Error_\tau(N) := \max_{t_0 \leq t \leq \Lambda t_0} \|u(t) - u_h^N(t)\|_{L^2(\Omega)}, \quad Error_h(t) := \|u(t) - u_h^N(t)\|_{L^2(\Omega)}.$$

While if the exact solution is unknown, we measure the temporal and spacial errors by using the same notations as above but defined as follows

$$Error_\tau(N) := \max_{t_0 \leq t \leq \Lambda t_0} \|u_h^{200}(t) - u_h^N(t)\|_{L^2(\Omega)}, \quad Error_h(t) = \|u_h^N(t) - u_{h/2}^N(t)\|_{L^2(\Omega)}.$$

Furthermore, we also use $\frac{\ln(Error_h/ Error_{h/2})}{\ln(2)}$ to measure the convergence order in space direction.

All of the numerical experiments are implemented by using Matlab 2018a on a PC with Intel(R) Core(TM) i7-7700 CPU @3.60GHz and 4.00GB RAM.

7.1. Example 1 (A scalar problem)

Here we aim to verify the spectral accuracy and high efficiency of CIM with the optimal parameters μ , α and the step-spacing τ been provided in Eq. (48). Firstly, we consider the scalar problem as follows:

$$K \frac{\partial u(t)}{\partial t} + \frac{1}{\Gamma(1-\beta)} \frac{\partial}{\partial t} \int_0^t (t-\tau)^{-\beta} (u(\tau) - u(0)) d\tau + au(t) = f(t) \text{ with } t > 0, u(0) = u_0, \quad (66)$$

and

$$f(t) = 1 + 3\sqrt{\pi}t + \frac{3\sqrt{\pi}(3-\beta)}{\Gamma(4-\beta)}t^{2-\beta} + \frac{3\sqrt{\pi}}{2}t^2,$$

$a = 1$, $u_0 = 1$. The exact solution is $u(t) = 1 + \frac{3\sqrt{\pi}}{2}t^2$.

Define the absolute error function w.r.t. N as

$$\text{Error}(N) := \max_{t_0 \leq t \leq \Lambda t_0} |u(t) - u^N(t)|.$$

The absolute errors of CIM for Problem (66) with different parameters Λ and fractional orders β are shown in Fig. 3.

One can see from Fig. 3 that the numerical results are consistent with the theoretical analysis in Theorem 3.3 and Theorem 3.4. That is, CIM has spectral accuracy, and the convergence order is $\mathcal{O}(\epsilon + e^{-cN})$ with $c = \mathcal{O}(1/\log(\Lambda))$. What is more, CIM is also unconditionally stable w.r.t. the fractional order β .

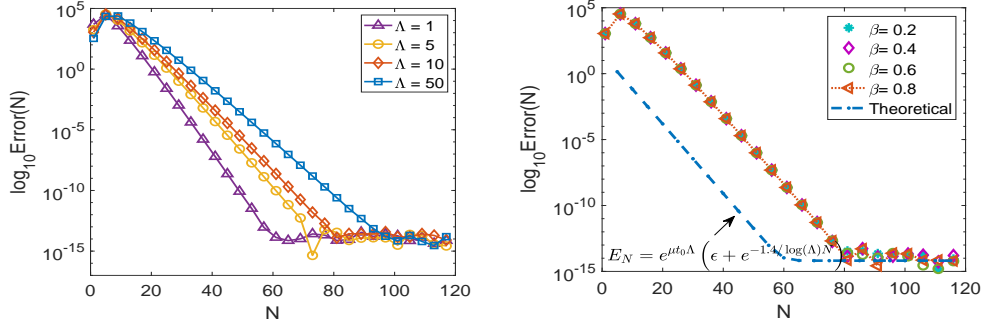


FIGURE 3. The numerical performance of CIM for Problem (66) at time $t = 0.6$. Left: The absolute numerical errors for different Λ with $\beta = 0.5$. Right: The absolute numerical errors for different β with $\Lambda = 10$.

7.2. Example 2 (A problem with vanishing initial data)

In this example, we consider that the initial value of the problem (1) is vanishing, and the exact solution is

$$u(x, t) = t^{3/2}x(1-x),$$

the source term is

$$f(x, t) = \frac{3}{2}Kt^{1/2}x(1-x) + \frac{3\sqrt{\pi}(5/2-\beta)}{4\Gamma(7/2-\beta)}t^{3/2-\beta}x(1-x) + 2t^{3/2}.$$

In this case, by choosing $\beta = 0.75$ and $\Lambda = 10$, the numerical performances of CIM-FEM are visually demonstrated in Fig. 4.

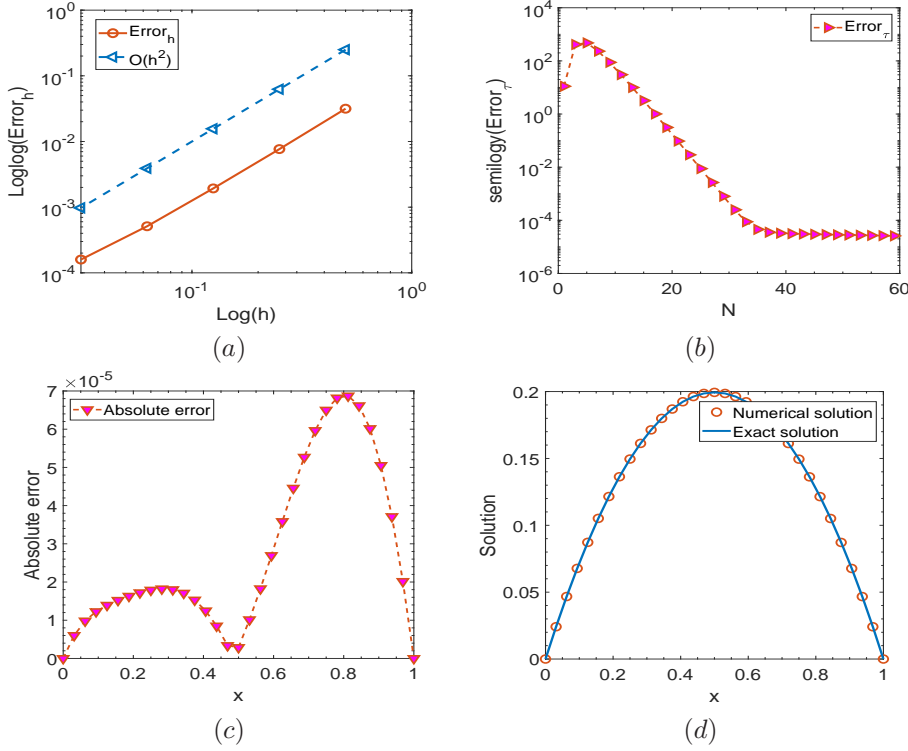


FIGURE 4. The numerical performance of CIM-FEM for Example 7.2 with vanishing initial value with $\beta = 0.75$ at time $t = 0.86$. (a) The spacial error Error_h with $N = 60$ and $h = 2^{-J}$, $J = 1, 2, 3, 4, 5$. (b) The temporal error Error_τ for different N with $h = 2^{-5}$. (c) The absolute error (i.e. $|u(x, t) - u_h^N|$) with $h = 2^{-5}$ and $N = 60$. (d) The fitting effect of the numerical solution with $h = 2^{-5}$ and $N = 60$.

We can see from Fig. 4 that convergence rate of CIM-FEM is $O(h^2)$ in space and spectral accuracy in time. In other words, the numerical results are consistent with the theoretical analysis given in Theorem 3.3, Theorem 4.3 and Theorem 5.2.

7.3. Example 3 (Two problems in one space dimension)

Here, we consider the 1-D homogeneous case of Problem (1) with non-smooth as well as smooth initial data, i.e., we choose the initial data as

$$(7.3.1) \quad u_0 = \pi^3 \chi_{(0, 3/4]}(x),$$

$$(7.3.2) \quad u_0 = \pi^3 x(1 - x),$$

respectively. It is clear that $u_0 \in L^2(\Omega)$ in (7.3.1) and $u_0 \in H_0^1(\Omega) \cap H^2(\Omega)$ in (7.3.2). To illustrate the accuracy of CIM, we take the numerical solution with $N = 200$ and $h = 1/2^7$ as the reference solution. The numerical results are showing in Tables 2-5.

More specifically, Table 2/Table 4 reflects the temporal errors Error_τ with non-smooth/smooth initial data; Table 3 and Table 5 are the corresponding spatial errors Error_h . These numerical results are consistent with the theoretical analyses in Theorem 3.3 with $f = 0$, Theorem 4.2, and Theorem 5.1.

TABLE 2. The temporal errors $Error_\tau$ for the homogeneous case of 1-D problem based on the non-smooth initial data (7.3.1) with $h = 1/2^7$ and $t = 0.8$.

$Error_\tau \backslash N$	20	40	60	80	100
β					
$\beta = 0.25$	2.2886E-02	9.8500E-05	9.5236E-09	3.8939E-14	3.4148E-14
$\beta = 0.50$	1.9995E-02	9.0973E-05	8.8491E-09	8.4586E-14	5.4752E-14
$\beta = 0.75$	1.5650E-02	9.0822E-05	7.0644E-09	6.7551E-14	6.9440E-14

TABLE 3. The spacial errors $Error_h$ for the homogeneous case of 1-D problem based on the non-smooth initial data (7.3.1) with $N = 100$ and $t = 0.8$.

1/M	$\beta = 0.25$		$\beta = 0.50$		$\beta = 0.75$	
	$Error_h$	Order	$Error_h$	Order	$Error_h$	Order
$1/2^5$	6.3098E-04	--	1.2092E-03	--	1.9769E-03	--
$1/2^6$	1.5809E-04	1.9969	3.0281E-04	1.9976	4.9514E-04	1.9974
$1/2^7$	3.9543E-05	1.9992	7.5735E-05	1.9994	1.2384E-04	1.9993
$1/2^8$	9.8872E-06	1.9998	1.8936E-05	1.9998	3.0964E-05	1.9998

TABLE 4. The temporal errors $Error_\tau$ for the homogeneous case of 1-D problem based on the smooth initial data (7.3.2) with $h = 1/2^7$ and $t = 0.8$.

$Error_\tau \backslash N$	20	40	60	80	100
β					
$\beta = 0.25$	5.3750E-03	2.3301E-05	2.1672E-09	6.1354E-14	9.3454E-15
$\beta = 0.50$	4.6838E-03	2.1532E-05	2.0118E-09	2.4407E-14	1.2485E-14
$\beta = 0.75$	3.6395E-03	2.1530E-05	1.5907E-09	1.4396E-14	1.5089E-14

TABLE 5. The spacial errors $Error_h$ for the homogeneous case of 1-D problem based on the smooth initial data (7.3.2) with $N = 100$ and $t = 0.8$.

1/M	$\beta = 0.25$		$\beta = 0.50$		$\beta = 0.75$	
	$Error_h$	Order	$Error_h$	Order	$Error_h$	Order
$1/2^5$	1.4943E-04	--	2.8646E-04	--	4.6867E-04	--
$1/2^6$	3.7484E-05	1.9951	7.1818E-05	1.9959	1.1749E-04	1.9960
$1/2^7$	9.3789E-06	1.9988	1.7967E-05	1.9990	2.9393E-05	1.9990
$1/2^8$	2.3452E-06	1.9997	4.4926E-06	1.9997	7.3495E-06	1.9998

7.4. Example 4 (Three problems in two space dimension)

In this example, we consider the 2-D homogeneous cases of Problem (1) with non-smooth as well as smooth initial values, i.e., we choose the initial data as

$$(7.4.1) \quad u_0 = \pi \chi_{(0,3/4] \times (0,1)}(x, y),$$

$$(7.4.2) \quad u_0 = 4\pi^2 xy(1-x)(1-y),$$

respectively. In addition, we also consider the inhomogeneous problem with vanishing initial data, that is

$$(7.4.3) \quad f(x, y, t) = 3\pi^5 e^{\frac{3}{2}t} \sin(x)(1-x)^2 y(y-1), \text{ and } u_0 = 0.$$

It is easy to find that the initial value in (7.4.1) belongs to $L^2(\Omega)$ and the initial value in (7.4.2) belongs to $H^2(\Omega) \cap H_0^1(\Omega)$. The numerical results are presented in Tables 6-11. Among them, Tables 6, 8 and 10 show the temporal numerical errors $Error_\tau$ for the three cases above; Tables 7, 9 and 11 illustrate the corresponding spatial errors $Error_h$. These numerical results verify Theorem 3.3, Theorem 4.3, Theorem 5.1 and Theorem 5.2.

TABLE 6. The temporal errors $Error_\tau$ for the homogeneous case of 2-D problem based on the non-smooth initial data (7.4.1) with $h = 1/2^5$ and $t = 0.6$.

$Error_\tau \backslash N$ β	20	40	60	80	100
$\beta = 0.25$	2.3321E-03	1.4808E-03	3.7972E-04	6.0484E-05	8.1762E-06
$\beta = 0.50$	3.2892E-03	1.6862E-03	3.0516E-04	5.3018E-05	7.8812E-06
$\beta = 0.75$	4.2886E-03	1.6947E-03	2.4295E-04	4.1240E-05	6.5707E-06

TABLE 7. The spacial errors $Error_h$ for the homogeneous case of 2-D problem based on the non-smooth initial data (7.4.1) with $N = 100$ and $t = 0.6$.

1/M	$\beta = 0.25$		$\beta = 0.50$		$\beta = 0.75$	
	$Error_h$	Order	$Error_h$	Order	$Error_h$	Order
$1/2^3$	1.6503E-03	--	1.8865E-03	--	2.0332E-03	--
$1/2^4$	3.9126E-04	2.0765	4.7358E-04	1.9941	5.5716E-04	1.8676
$1/2^5$	9.6537E-05	2.0190	1.1877E-04	1.9955	1.4253E-04	1.9668
$1/2^6$	2.4044E-05	2.0054	2.9700E-05	1.9996	3.5821E-05	1.9924

TABLE 8. The temporal errors $Error_\tau$ for the homogeneous case of 2-D problem based on the smooth initial data (7.4.2) with $h = 1/2^5$ and $t = 0.6$.

$Error_\tau \backslash N$ β	20	40	60	80	100
$\beta = 0.25$	1.1401E-03	6.8451E-04	1.6312E-04	2.5065E-05	3.4184E-06
$\beta = 0.50$	1.6228E-03	7.6423E-04	1.2958E-04	2.2021E-05	3.2967E-06
$\beta = 0.75$	2.1277E-03	7.4689E-04	1.0162E-04	1.7137E-05	2.7505E-06

TABLE 9. The spacial errors $Error_h$ for the homogeneous case of 2-D problem based on the smooth initial data (7.4.2) with $N = 100$ and $t = 0.6$.

1/M	$\beta = 0.25$		$\beta = 0.50$		$\beta = 0.75$	
	$Error_h$	Order	$Error_h$	Order	$Error_h$	Order
$1/2^3$	7.2485E-04	--	7.4908E-04	--	6.8250E-04	--
$1/2^4$	1.5771E-04	2.2004	1.5307E-04	2.2909	1.2654E-04	2.4312
$1/2^5$	3.7754E-05	2.0626	3.5949E-05	2.0902	2.8830E-05	2.1340
$1/2^6$	9.3307E-06	2.0166	8.8396E-06	2.0239	7.0319E-06	2.0356

TABLE 10. The temporal errors $Error_\tau$ for the inhomogeneous case of 2-D problem based on the source term (7.4.3) with $u_0 = 0$, $h = 1/2^5$ and $t = 0.6$.

$Error_\tau \backslash N$ β	20	40	60	80	100
$\beta = 0.25$	7.5385E-02	4.3031E-02	2.2798E-02	8.9194E-03	3.2602E-03
$\beta = 0.50$	9.4276E-02	4.7014E-02	2.0328E-02	8.3595E-03	3.2009E-03
$\beta = 0.75$	1.1184E-01	4.7663E-02	1.8007E-02	7.3730E-03	2.9225E-03

7.5. Example 5 (Numerical performance of the acceleration algorithm)

This example targets on verifying the numerical effectiveness of the acceleration algorithm developed in Section 6. Here, “CIM-FEM” indicates that the designed numerical scheme is implemented directly without interpolation acceleration; “CIM-Int-FEM” represents that the algorithm uses interpolation approximation to

TABLE 11. The spacial errors $Error_h$ for the inhomogeneous case of 2-D problem based on the source term (7.4.3) with $u_0 = 0$, $N = 100$ and $t = 0.6$.

$1/M$	$\beta = 0.25$		$\beta = 0.50$		$\beta = 0.75$	
	$Error_h$	$Order$	$Error_h$	$Order$	$Error_h$	$Order$
$1/2^3$	1.0311E-02	--	1.4646E-02	--	1.8830E-02	--
$1/2^4$	2.6138E-03	1.9799	3.7230E-03	1.9760	4.7974E-03	1.9727
$1/2^5$	6.5389E-04	1.9990	9.3200E-04	1.9980	1.2016E-03	1.9973
$1/2^6$	1.6346E-04	2.0001	2.3303E-04	1.9998	3.0048E-04	1.9996

improve the computational speed (see Section 6). We use these two algorithms to revisit Example 7.2, and the numerical results are shown in Table 12.

To show the efficiency of the acceleration algorithm CIM-Int-FEM more clearly, we choose the spatial step-spacing as $\frac{1}{2^5}$, $\frac{1}{2^6}$, $\frac{1}{2^7}$, $\frac{1}{2^8}$, and $\frac{1}{2^9}$, and compare the numerical results of CIM-FEM and CIM-Int-FEM in Table 12.

TABLE 12. The CPU time of CIM-FEM and CIM-Int-FEM for the 1-D homogeneous problem based in the non-smooth initial data (7.3.1) with $N = 100$, $n = 16$, $t = 0.86$, and $\beta = 0.75$.

$1/M$	CIM-FEM		CIM-Int-FEM		IAR
	CPU-time	$Error_h$	CPU-time	$Error_h$	
$h = 1/2^5$	7.0476E-01s	1.2233E-03	1.8388E-01s	4.7294E-03	6.5215E-03
$h = 1/2^6$	1.3580E+00s	1.2777E-03	3.1009E-01s	4.6669E-03	4.5505E-03
$h = 1/2^7$	2.7474E+00s	1.2917E-03	5.7774E-01s	4.6514E-03	3.2070E-03
$h = 1/2^8$	5.2977E+00s	1.2952E-03	1.3814E+00s	4.6475E-03	2.2658E-03
$h = 1/2^9$	1.0691E+01s	1.2961E-03	2.1793E+00s	4.6465E-03	1.6018E-03

We choose the number of the interpolation nodes as $n = 16$. As one can see from Table 12, CIM-Int-FEM and CIM-FEM have similar accuracy, but the CPU time of the algorithm before interpolation is about 5 times as long as after interpolation, which achieves our goal of acceleration. Also, one can observe from IAR (the interpolation approximation rates) that the CIM-Int-FEM algorithm is effective.

In a short, the above examples verify that both of the schemes CIM-Int-FEM and CIM-FEM we proposed are effective. The spatial finite element discretization can reach to the optimal second-order convergence and the time CIM discretization has spectral accuracy. The improved acceleration interpolation process is significant.

8. CONCLUSIONS

In this paper, the time fractional subdiffusion-normal transport model, which depicts a crossover from sub-diffusion (as $t \rightarrow 0$) to normal diffusion (as $t \rightarrow \infty$), is analyzed and numerically solved. First, based on the analytic properties of the bivariate Mittag-Leffler function, we rigorously discuss the regularity, existence and uniqueness of the model solution of the homogeneous as well as inhomogeneous cases. In particular, new regularity results show that, with time developing, the time regularity of the solution to TFDEs is dominated by the highest-order operator. Then, a numerical scheme with high-precision and low regularity requirements is developed. More specifically, for time discretization, by Laplace transform, a parallel CIM scheme is designed, in which the hyperbolic integral contour is selected; for space discretization, the standard Galerkin finite element method is employed. Error estimates show that CIM-FEM has spectral accuracy in time and can reach to optimal second-order convergence with smooth as well as non-smooth initial data in space. Furthermore, the barycentric interpolation algorithm is proposed to accelerate the algorithm, and the error estimate shows that the convergence rate of this interpolation is remarkably fast. Several numerical experiments in 1-D and 2-D for both homogeneous and inhomogeneous cases verify all of the theoretical results. High numerical performances of these numerical examples also illustrate the high efficiency and robustness of our numerical schemes.

ACKNOWLEDGMENTS

The authors Ma and Deng are supported by the National Natural Science Foundation of China under Grant No. 12071195, the AI and Big Data Funds under Grant No. 2019620005000775, and the Innovative Groups of Basic Research in Gansu Province under Grant No.22JR5RA391. The author Zhao is supported by Guangdong Basic and Applied Basic Research Foundation under Grant No. 2022A15150 11332.

APPENDIX A

A.1 The definition of the multivariate Mittag-Leffler function

Let $\alpha, \beta, \gamma \in \mathbb{C}$, and $\operatorname{Re}(\alpha) > 0, \operatorname{Re}(\beta) > 0$. The bivariate Mittag-Leffler function is defined as

$$E_{(\alpha, \beta), \gamma}^{\delta}(z_1, z_2) := \sum_{k=0}^{\infty} \sum_{l=0}^{\infty} \frac{(\delta)_{k+l}}{\Gamma(\alpha k + \beta l + \gamma)} \cdot \frac{z_1^k z_2^l}{k!l!}, \quad (67)$$

where the numerator $(\delta)_{k+l}$ is the Pochhammer symbol, i.e.,

$$(a)_n = \frac{\Gamma(a+n)}{\Gamma(a)} = a(a+1)(a+2)\dots(a+n-1).$$

A.2 The proof of Lemma 2.3

Proof. Let R_x and R_y be the associated radii of convergence of the double power series. That is, $\sum_{m,n=0}^{\infty} C_{m,n} x^m y^n$ is convergent for $|x| < R_x$ and $|y| < R_y$. Denote $C_{k,l} = \frac{(\delta)_{k+l}}{\Gamma(\alpha k + \beta l + \gamma) k! l!}$. According to the definition of the bivariate Mittag-Leffler function defined in (67), its associated radii of convergence are

$$R_x := \limsup_{\substack{k \rightarrow \infty \\ l \rightarrow \infty}} \frac{|C_{k,l}|}{|C_{k+1,l}|}, \quad R_y := \limsup_{\substack{k \rightarrow \infty \\ l \rightarrow \infty}} \frac{|C_{k,l}|}{|C_{k,l+1}|}.$$

Recall that the asymptotic formula (see [42, (3.1.3)])

$$\frac{\Gamma(z+a)}{\Gamma(z+b)} = z^{a-b} \left[1 + \frac{(a-b)(a-b-1)}{2z} + \mathcal{O}\left(\frac{1}{z^2}\right) \right] \quad \text{with } z \rightarrow \infty, \quad |\arg(z)| < \pi.$$

By the aforementioned asymptotic formula, there holds

$$\begin{aligned} R_x &= \limsup_{\substack{k \rightarrow \infty \\ l \rightarrow \infty}} \frac{|C_{k,l}|}{|C_{k+1,l}|} = \limsup_{\substack{k=\vartheta t, l=vt, \\ t \rightarrow \infty}} \frac{|C_{\vartheta t, vt}|}{|C_{\vartheta t+1, vt}|} = \limsup_{t \rightarrow \infty} \left| \frac{\Gamma(\alpha \vartheta t + \beta vt + \alpha + \gamma)}{\Gamma(\alpha \vartheta t + \beta vt + \gamma)} \right| \cdot \frac{|\vartheta t + 1|}{|\delta + \vartheta t + vt|} \\ &= \limsup_{t \rightarrow \infty} \left| (\alpha \vartheta t + \beta vt)^{\alpha} \left(1 + \frac{\alpha(\alpha-1)}{2(\alpha \vartheta t + \beta vt)} + \mathcal{O}\left(\frac{1}{(\alpha \vartheta t + \beta vt)^2}\right) \right) \right| \cdot \frac{|\vartheta t + 1|}{|\delta + \vartheta t + vt|}. \end{aligned} \quad (68)$$

Choose v and ϑ , which satisfy $\frac{|v\beta|}{|\vartheta\alpha|} < 1$ ($\frac{|\vartheta\alpha|}{|v\beta|} < 1$ for R_y). Since $\ln(1+z) = z - \frac{z^2}{2} + \frac{z^3}{3} - \dots$ ($z \in \mathbb{C}$ with $|z| < 1$), by writing $\alpha = r_1 e^{i\theta_1}$, $\beta = r_2 e^{i\theta_2}$, we have

$$\begin{aligned}
& (\alpha\vartheta t + \beta vt)^\alpha \\
&= \exp\left(r_1 e^{i\theta_1} \ln(\vartheta t r_1 e^{i\theta_1} + v t r_2 e^{i\theta_2})\right) \\
&= \exp\left(r_1 e^{i\theta_1} \left(\ln(\vartheta t r_1 e^{i\theta_1}) + \ln\left(1 + \frac{v r_2}{\vartheta r_1} e^{i(\theta_2 - \theta_1)}\right)\right)\right) \\
&\simeq \exp\left(r_1 (\cos \theta_1 + i \sin \theta_1) (\ln(\vartheta t r_1) + i\theta_1)\right) \exp\left(\frac{v r_2}{\vartheta} e^{i\theta_2}\right) \\
&= \exp\left(r_1 \cos \theta_1 \ln(\vartheta t r_1) + \frac{v r_2}{\vartheta} \cos \theta_2 - \theta_1 r_1 \sin \theta_1\right) \cdot \exp\left(i r_1 \theta_1 \cos \theta_1 + i \sin \theta_1 \ln(\vartheta t r_1) + i \frac{v r_2}{\vartheta} \sin \theta_2\right).
\end{aligned} \tag{69}$$

By Eqs. (68) and (69), leaving out the small quantity and by the boundness of $\frac{|\vartheta t + 1|}{|\delta + \vartheta t + vt|}$, we get $R_x \rightarrow \infty$ when $\text{Re}(\alpha) = r_1 \cos \theta_1 > 0$, $t \rightarrow \infty$. Similarly, we can also get $R_y \rightarrow \infty$ when $\text{Re}(\beta) = r_2 \cos \theta_2 > 0$, $t \rightarrow \infty$. That is, when $\text{Re}(\alpha) > 0$ and $\text{Re}(\beta) > 0$, the double power series in Eq. (67) is convergence uniformly for all $z_1, z_2 \in \mathbb{C}$. Finally, by the definition of an entire function (cf. [42, Appendix B]), one can get the desired result. \square

A.3 The proof of Lemma 2.4

Proof. Let $\alpha, \beta, \gamma, \omega_1, \omega_2 \in \mathbb{R}$ with $0 < \alpha < \beta \leq 1$, $\gamma \geq 0$ and $\omega_1, \omega_2 < 0$. Firstly, for $t = 0$, according to the series representation of the bivariate Mittag-Leffler function in Eq. (67), there exist a positive constant C such that

$$\left|E_{(\alpha, \beta), \gamma}^1(\omega_1 t^\alpha, \omega_2 t^\beta)\right| = \frac{1}{\Gamma(\gamma)} \leq C. \tag{70}$$

For $t > 0$, by Corollary 2 in [41], the contour integral representation of the bivariate Mittag-Leffler function $E_{(\alpha, \beta), \gamma}^1(\omega_1 t^\alpha, \omega_2 t^\beta)$ is

$$E_{(\alpha, \beta), \gamma}^1(\omega_1 t^\alpha, \omega_2 t^\beta) = \frac{t^{1-\gamma}}{2\pi i} \int_{\Gamma_{\theta, \delta}} \frac{e^{zt} z^{-\gamma}}{1 + |\omega_1| z^{-\alpha} + |\omega_2| z^{-\beta}} dz. \tag{71}$$

Case I: for given $\beta \in (0, 1)$ and any $\alpha \in (0, 1)$ with $0 < \alpha < \beta < 1$. When $z \in \Gamma_{\theta, \delta}$, we choose $\theta \in (\frac{\pi}{2}, \pi)$, which only depends on β and closes to $\frac{\pi}{2}$ enough such that $\arg(|\omega_2| z^{-\beta}) > -\frac{\pi}{2}$. Then the angle between $|\omega_2| z^{-\beta}$ and $1 + |\omega_1| z^{-\alpha}$ is less than $\pi/2$ and the denominator in (71) satisfies

$$|1 + |\omega_1| z^{-\alpha} + |\omega_2| z^{-\beta}| \geq |\omega_2| |z|^{-\beta} \cos \beta \theta. \tag{72}$$

Based on these, choosing $\delta = 1/t > 0$ large enough, then we get

$$\begin{aligned}
\left|E_{(\alpha, \beta), \gamma}^1(\omega_1 t^\alpha, \omega_2 t^\beta)\right| &\leq \frac{t^{1-\gamma}}{2\pi} \int_{\Gamma_{\theta, \delta}} \frac{e^{|z|t} |z|^{-\gamma}}{|1 + |\omega_1| z^{-\alpha} + |\omega_2| z^{-\beta}|} |dz| \leq \frac{t^{1-\gamma}}{2\pi |\omega_2| \cos \beta \theta} \int_{\Gamma_{\theta, \delta}} e^{|z|t} |z|^{\beta-\gamma} |dz| \\
&\leq \frac{t^{1-\gamma}}{2\pi |\omega_2| \cos \beta \theta} C t^{\gamma-1-\beta} \leq \frac{C}{|\omega_1 t^\beta|}.
\end{aligned}$$

Case II: for given $\alpha \in (0, 1)$, $\beta = 1$. Similar to (i), when $z \in \Gamma_{\theta, \delta}$, by choosing $\theta \in (\frac{\pi}{2}, \pi)$, which depends on α and closes to $\frac{\pi}{2}$ enough such that $\alpha\theta + \arg(1 + |\omega_2| z^{-1}) \geq -\frac{\pi}{2}$. In this case, the denominator in (71) satisfies

$$|1 + |\omega_2| z^{-1} + |\omega_1| z^{-\alpha}| > |1 + |\omega_2| z^{-1}| \geq |\omega_2| |z|^{-1} \cos\left(\theta - \frac{\pi}{2}\right). \tag{73}$$

Similarly, there holds

$$\begin{aligned} \left| E_{(\alpha, \beta), \gamma}^1(\omega_1 t^\alpha, \omega_2 t^\beta) \right| &\leq \frac{t^{1-\gamma}}{2\pi} \int_{\Gamma_{\theta, \delta}} \frac{e^{|z|t}|z|^{-\gamma}}{|1 + |\omega_1|z^{-\alpha} + |\omega_2|z^{-\beta}|} |dz| \leq \frac{t^{1-\gamma}}{2\pi |\omega_2| \sin \theta} \int_{\Gamma_{\theta, \delta}} e^{|z|t}|z|^{1-\gamma} |dz| \\ &\leq \frac{t^{1-\gamma}}{2\pi |\omega_2| \sin \theta} C t^{\gamma-1-1} \leq \frac{C}{|\omega_2 t|}. \end{aligned}$$

Thus the proof of this lemma is completed. \square

APPENDIX B

The proof of Proposition 3.2

Proof. By Eq. (39), we see that $z'(\phi) = i\mu \cos(i\phi - \alpha)$. According to the definition of $v(t, r, \phi)$ in Eq. (41), when we take ϕ in the top half of S , i.e., $\phi = x + iy \in S$ with $0 < y < \tilde{d}$ and $0 < \alpha - \tilde{d} < \alpha + \tilde{d} < \pi/2 - \delta'$, there holds

$$v(t, r, x + iy) = \frac{\mu}{2\pi} e^{\mu(1 - \sin(\alpha + y - ix))t} \cos(\alpha + y - ix) \hat{u}(\mu(1 - \sin(\alpha + y - ix))).$$

Let $l' = \alpha + y < \alpha + \tilde{d}$. Taking L^2 -norm on the above equation, we get

$$\|v(t, r, x + iy)\|_{L^2(\Omega)} \leq \frac{\mu}{2\pi} e^{\mu t(1 - \sin l' \cosh x)} \|\cos(l' - ix) \hat{u}(\mu(1 - \sin(l' - ix)))\|_{L^2(\Omega)}. \quad (74)$$

Further, by (45) and (74), we have

$$\|\cos(l' - ix) \hat{u}(\mu(1 - \sin(l' - ix)))\|_{L^2(\Omega)} \leq \frac{C |\cos(l' - ix)|}{|\mu(1 - \sin(l' - ix))|} \left(\|u_0\|_{L^2(\Omega)} + \|\hat{f}(z)\|_{N_r} \right). \quad (75)$$

Note that

$$\frac{|\cos(l' - ix)|}{|\mu(1 - \sin(l' - ix))|} \leq \frac{1}{\mu} \sqrt{\frac{1 + \sin l'}{1 - \sin l'}}, \quad (76)$$

by Inequalities (74)-(76), we can obtain that

$$\|v(t, r, x + iy)\|_{L^2(\Omega)} \leq C e^{\mu t} \sqrt{\frac{1 + \sin(\alpha + \tilde{d})}{1 - \sin(\alpha + \tilde{d})}} \left(\|u_0\|_{L^2(\Omega)} + \|\hat{f}(z)\|_{N_r} \right) e^{-\mu t \sin(\alpha - \tilde{d}) \cosh x}. \quad (77)$$

The estimate of $v(t, r, \phi)$ in the lower part of S , where $\phi = x - iy \in S$ with $-\tilde{d} < -y \leq 0$, follows by analogy. In fact, due to $\sin(\alpha - y) < \sin \alpha < \sin(\alpha + y)$, it follows that

$$\|v(t, r, x - iy)\|_{L^2(\Omega)} \leq C e^{\mu t} \sqrt{\frac{1 + \sin(\alpha + \tilde{d})}{1 - \sin(\alpha + \tilde{d})}} \left(\|u_0\|_{L^2(\Omega)} + \|\hat{f}(z)\|_{N_r} \right) e^{-\mu t \sin(\alpha - \tilde{d}) \cosh x}. \quad (78)$$

Thus, for all $\phi = x \pm iy \in S$, the integrand $v(t, r, \phi)$ satisfies the following consistent estimate:

$$\|v(t, r, \phi)\|_{L^2(\Omega)} \leq C e^{\mu t} \varphi(\alpha, \tilde{d}) \left(\|u_0\|_{L^2(\Omega)} + \|\hat{f}(z)\|_{N_r} \right) e^{-\mu t \sin(\alpha - \tilde{d}) \cosh x},$$

where $\varphi(\alpha, \tilde{d}) = \sqrt{\frac{1 + \sin(\alpha + \tilde{d})}{1 - \sin(\alpha + \tilde{d})}}$. Therefore, the proof of this proposition is completed. \square

REFERENCES

- [1] A. A. Kilbas, H. M. Srivastava, and J. J. Trujillo, *Theory and Applications of Fractional Differential Equations*. Elsevier, Amsterdam, 2006.
- [2] L. C. Evans, *Partial Differential Equations*. Second Edition. American Mathematical Society, Providence, Rhode Island, 2010.
- [3] I. Podlubny, *Fractional Differential Equations*. Academic press, San Diego, 1999.
- [4] Z. Q. Chen, Time fractional equations and probabilistic representation. *Chaos Solitons Fractals*, 102 (2017): 168-174.
- [5] B. Toaldo, Convolution-type derivatives, hitting-times of subordinators and time-changed C_0 -semigroups. *Potential Anal.*, 42 (2015) :115-140
- [6] A. Kubica and M. Yamamoto, Initial-boundary value problems for fractional diffusion equations with time-dependent coefficients. *Fract. Calc. Appl. Anal.*, 21 (2018): 276-311.
- [7] K. Sakamoto and M. Yamamoto, Initial value/boundary value problems for fractional diffusion-wave equation and application to some inverse problems, *J. Math. Anal. Appl.*, 382 (2011): 426-447.
- [8] R. Metzler and J. Klafter, The random walk's guide to anomalous diffusion: a fractional dynamics approach. *Phys. Rep.*, 339 (2000): 1-77.
- [9] R. Metzler and J. Klafter, The restaurant at the end of the random walk: recent developments in the description of anomalous transport by fractional dynamics. *J. Phys. A: Math. Gen.*, 37 (2004): 161-208.
- [10] R. Schumer, D. A. Benson, M. M. Meerschaert, and B. Baeumer, Fractal mobile/immobile solute transport, *Water Resour. Res.*, 39 (2003): 1296.
- [11] Y. Zhang, C. Green, and B. Baeumer, Linking aquifer spatial properties and non-Fickian transport in mobile-immobile like alluvial settings, *J. Hydrol.*, 512 (2014): 315-331.
- [12] B. T. Jin, B. Y. Li, and Z. Zhou, Numerical analysis of nonlinear subdiffusion equations. *SIAM J. Numer. Anal.*, 56 (2018): 1-23.
- [13] B. T. Jin, R. Lazarov, and Z. Zhou, An analysis of the L1 scheme for the subdiffusion equation with nonsmooth data. *IMA J. Numer. Anal.*, 36 (2016): 197-221.
- [14] B. T. Jin, R. Lazarov, Y. K. Liu, and Z. Zhou, The Galerkin finite element method for a multi-term time-fractional diffusion equation. *J. Comput. Phys.*, 281 (2015): 852-843.
- [15] G. H. Gao, Z. Z. Sun, and H. W. Zhang, A new fractional numerical differentiation formula to approximate the Caputo fractional derivative and its applications. *J. Comput. Phys.*, 259 (2014): 33-50.
- [16] Y. M. Lin and C. J. Xu, Finite difference/spectral approximations for the time-fractional diffusion equation. *J. Comput. Phys.*, 225 (2007): 1533-1552.
- [17] C. Lubich, Discretized fractional calculus. *SIAM J. Math. Anal.*, 17 (1986): 704-719.
- [18] C. Lubich, I. H. Sloan, and V. Thomée, Nonsmooth data error estimates for approximations of an evolution equation with a positive-type memory term. *Math. Comp.*, 65 (1996): 1-17.
- [19] E. Cuesta, C. Lubich, and C. Palencia, Convolution quadrature time discretization of fractional diffusion-wave equations. *Math. Comp.*, 75 (2006): 673-696.
- [20] F. H. Zeng, C. P. Li, F. W. Liu, and I. Turner, Numerical algorithms for time-fractional subdiffusion equation with second-order accuracy. *SIAM J. Sci. Comput.*, 37 (2015): A55-A78.
- [21] Y. G. Yan, Z. Z. Sun, and Z. M. Zhang, Fast evaluation of the Caputo fractional derivative and its applications to fractional diffusion equations: a second-order scheme. *Commun. Comput. Phys.*, 22 (2017): 1028-1048.
- [22] S. D. Jiang, J. W. Zhang, Q. Zhang, and Z. M. Zhang, Fast evaluation of the Caputo fractional derivative and its applications to fractional diffusion equations. *Commun. Comput. Phys.*, 21 (2017): 650-678.
- [23] X. Li, H. L. Liao, and L. M. Zhang, A second-order fast compact scheme with unequal time-steps for subdiffusion problems. *Numer. Algorithms*, 86 (2021): 1011-1039.
- [24] M. Stynes, E. O'Riordan, and J. L. Gracia, Error analysis of a finite difference method on graded meshes for a time-fractional diffusion equation. *SIAM J. Numer. Anal.*, 55 (2017): 1057-1079.
- [25] M. L. Fernández and C. Palencia, On the numerical inversion of the Laplace transform of certain holomorphic mappings. *Appl. Numer. Math.*, 51 (2004): 289-303.
- [26] M. L. Fernández, C. Palencia, and A. Schädle, A spectral order method for inverting sectorial Laplace transforms. *SIAM J. Numer. Anal.*, 44 (2006): 1332-1350.
- [27] W. Mclean and V. Thomée, Time discretization of an evolution equation via Laplace transforms. *IMA J. Numer. Anal.*, 24 (2004): 439-463.
- [28] W. Arendt, Charles J.K. Batty, M. Hieber, and F. Neubrander, *Vector-valued Laplace Transforms and Cauchy Problems*. Springer-Verlag, Berlin, 2011.
- [29] R. Piessens, A bibliography on numerical inversion of the Laplace transform and applications. *J. Comput. Appl. Math.*, 1 (1975): 115-128.
- [30] R. Piessens and N. D. P. Dang, A bibliography on numerical inversion of the Laplace transform and applications: A supplement. *J. Comput. Appl. Math.*, 2 (1976): 225-228.
- [32] W. A. Essah and L. M. Delves, On the numerical inversion of the Laplace transform. *Inverse Probl.*, 4 (1988): 705-724.

- [31] A. Talbot, The accurate numerical inversion of Laplace transforms. *IMA J. Appl. Math.*, 23 (1979): 97-120.
- [32] D. Sheen, I. H. Sloan, and V. Thomée, A parallel method for time-discretization of parabolic problems based on contour integral representation and quadrature. *Math. Comp.*, 69 (2000): 177-195.
- [33] J. P. Berrut and L. N. Trefethen, Barycentric Lagrange interpolation. *SIAM Rev.*, 46 (2004): 501-517.
- [34] V. Thomée, *Galerkin Finite Element Methods for Parabolic Problems*. Springer-Verlag, Berlin, 2006.
- [35] W. H. Deng, B. Y. Li, Z. Qian, and H. Wang, Time discretization of a tempered fractional Feynman-Kac equation with measure data. *SIAM J. Numer. Anal.*, 56 (2018): 3249-3275.
- [36] W. H. Deng, Finite element method for the space and time fractional Fokker-Planck equation. *SIAM J. Numer. Anal.*, 47 (2008): 204-226.
- [37] W. H. Deng and Z. J. Zhang, *High Accuracy Algorithm for the Differential Equations Governing Anomalous Diffusion: Algorithm and Models for Anomalous Diffusion*. World Scientific, Singapore, 2019.
- [38] Yu. Luchko, Operational method in fractional calculus. *Fract. Calc. Appl. Anal.*, 2 (1999): 463-488.
- [39] K. Mustapha, An L_1 approximation for a fractional reaction-diffusion equation, a second-order error analysis over time-grade meshes, *SIAM J. Numer. Anal.*, 58 (2020): 1319-1338.
- [40] M. F. She, D. F. Li, and H. W. Sun, A transformed L_1 method for solving the multi-term time-fractional diffusion problem, *Math. Comput. Simulat.*, 193 (2022): 584-606.
- [41] A. Fernandez, C. Kürt, and M. A. Özarslan, A naturally emerging bivariate Mittag-Leffler function and associated fractional-calculus operators, *Comput. Appl. Math.*, 39 (2020): 200.
- [42] R. Gorenflo, A. A. Kilbas, F. Mainardi, and S. V. Rogosin, *Mittag-Leffler Functions, Related Topics and Applications*. Springer-Verlag Berlin Heidelberg, 2010.
- [43] J. Mu, B. Ahmadc, and S. B. Huang, Existence and regularity of solutions to time-fractional diffusion equations. *Comput. Math. Appl.*, 73 (2017): 985-996.
- [44] Z. Y. Zheng and Y. M. Wang, An averaged L_1 -type compact difference method for time-fractional mobile/immobile diffusion equations with weakly singular solutions. *Appl. Math. Lett.*, 131 (2022): 108076.
- [45] O. Nikana, J. A. Tenreiro Machadob, A. Golbabaia, and T. Nikazada, Numerical approach for modeling fractal mobile/immobile transport model in porous and fractured media. *Int. Commun. Heat. Mass.*, 111 (2020): 104443.
- [46] B. Fornberg, *A Practical Guide to Pseudospectral Methods*, Cambridge University Press, Cambridge, UK, 1996.
- [47] Lloyd N. Trefethen, *Spectral Methods in Matlab*, SIAM, Philadelphia, 2000.